

# FROST ACTION PREDICTIVE TECHNIQUES FOR ROADS AND AIRFIELDS

PB88 - 144050



Research, Development,  
and Technology

Turner-Fairbank Highway  
Research Center  
6300 Georgetown Pike  
McLean, Virginia 22101-2296



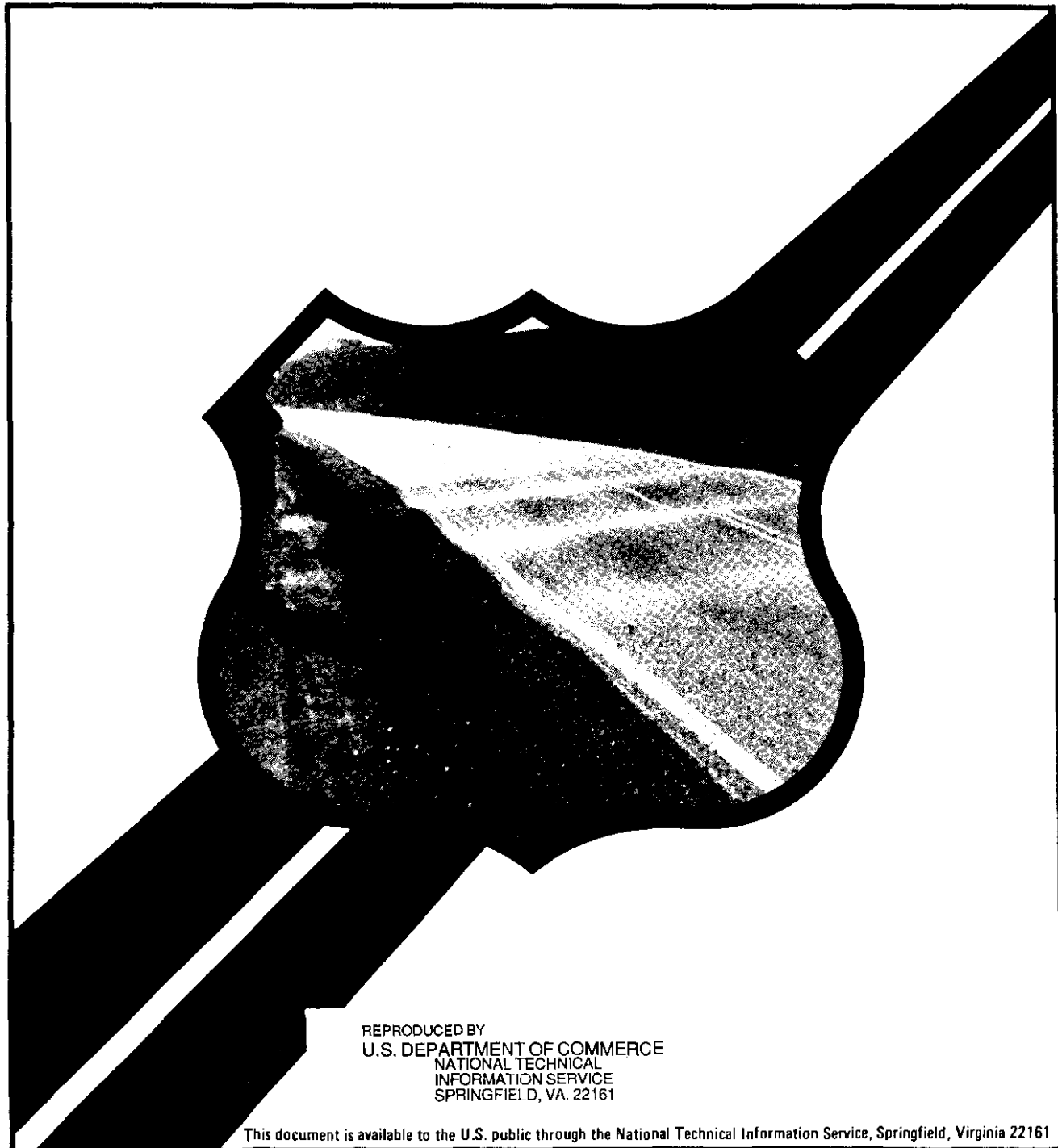
U.S. Department  
of Transportation

**Federal Highway  
Administration**

## VOL. I: A COMPREHENSIVE SURVEY OF RESEARCH FINDINGS

Report No.  
FHWA/RD-87/057

Final Report  
June 1987




REPRODUCED BY  
U.S. DEPARTMENT OF COMMERCE  
NATIONAL TECHNICAL  
INFORMATION SERVICE  
SPRINGFIELD, VA. 22161

This document is available to the U.S. public through the National Technical Information Service, Springfield, Virginia 22161

## FOREWORD

This report presents the results of six years of intensive research to advance the state of knowledge and the ability to predict the effects of frost action on pavement performance. The two principal effects of frost are heave, causing pavement roughness, and thaw weakening of the subgrade materials, causing adverse pavement deformations and accelerated pavement cracking. Analytical and laboratory test methods were developed and successfully tested against field measurements. Details of the investigations have been documented in several research reports, for which citations are given throughout the report.

This report will be of interest to pavement design and geotechnical engineers concerned with pavement distress in seasonal frost areas. Sufficient copies of the report are being distributed by FHWA Bulletin to provide a minimum of two copies to each FHWA regional and division office, and two copies to each State highway agency. Direct distribution is being made to division offices.



Richard E. Hay, Director  
Office of Engineering and Highway  
Operations Research and Development

## NOTICE

This document is disseminated under the sponsorship of the Department of Transportation in the interest of information exchange. The United States Government assumes no liability for its contents or use thereof.

The contents of this report reflect the views of the contractor, who is responsible for the accuracy of the data presented herein. The contents do not necessarily reflect the official policy of the Department of Transportation. This report does not constitute a standard, specification, or regulation.

The United States Government does not endorse products or manufacturers. Trade or manufacturers names appear herein only because they are considered essential to the object of this document.

1. Report No. FHWA/RD-87/057		2. Government Accession No.		3. Recipient's Catalog No. PB88.144050	
4. Title and Subtitle Frost Action Predictive Techniques for Roads and Airfields: Vol. I: A Comprehensive Survey of Research Findings				5. Report Date June 1987	
7. Author's: T. C. Johnson, R. L. Berg, E. J. Chamberlain, and D. M. Cole				6. Performing Organization Code	
9. Performing Organization Name and Address U. S. Army Cold Regions Research and Engineering Laboratory 72 Lyme Road Hanover, New Hampshire 03755-1290				8. Performing Organization Report No. 86-18	
12. Sponsoring Agency Name and Address Office of Engineering and Highway Operations Research and Development Federal Highway Administration 6300 Georgetown Pike, McLean, VA 22101				10. Work Unit No. (TRAINS) NCP 3E3b0992	
				11. Contract or Grant No. P. O. 8-3-0187	
15. Supplementary Notes FHWA Contract Manager (COTR): Albert F. DiMillio (HMR-30) The research was co-sponsored by: Office of the Chief of Engineers, U. S. Army Federal Aviation Administration				13. Type of Report and Period Covered Final Report October 1978 - December 1985	
14. Sponsoring Agency Code CME/0285					
16. Abstract  Findings from a six-year field and laboratory program of frost-action research in four principal areas are summarized. Research on the first topic, frost-susceptibility index tests, led to selection of the Corps of Engineers' frost design soil classification system as a useful method at the simplest level of testing. At a much more complex level, a new freezing test combined with a CBR test after thawing is recommended as an index of susceptibility to both frost heave and thaw weakening. Under the second topic, a soil column and dual gamma system were developed and applied to obtain soil data used in improving and validating a mathematical model of frost heave, the objective of the third research topic. The model was effectively improved, a probabilistic component was added, and it was successfully tested against field and laboratory measurements of frost heave. A thaw consolidation algorithm was added, which was shown to be useful in predicting the seasonal variation in resilient modulus of granular soils, the objective of the fourth topic. A laboratory testing procedure was developed for assessing the resilient modulus of thawed soil at various stages of the recovery process, as a function of the applied stress and the soil moisture tension, which increases as the soil gradually desaturates during recovery. The procedure was validated by means of appropriate analyses of deflections measured on pavements by a falling-weight deflectometer. Frameworks for implementing findings from the principal research topics are outlined.					
17. Key Words Freezing-thawing      Resilient Modulus Frost Action Frost Heave Frost Susceptibility Thaw weakening			18. Distribution Statement This document is available to the public through the National Technical Information Service, Springfield, Virginia 22161.		
19. Security Classif. (of this report) Unclassified		20. Security Classif. (of this page) Unclassified		21. No. of Pages 53	22. Price AD4 14.95

12

# METRIC (SI\*) CONVERSION FACTORS

## APPROXIMATE CONVERSIONS TO SI UNITS

Symbol	When You Know	Multiply By	To Find	Symbol
--------	---------------	-------------	---------	--------

### LENGTH

in	inches	2.54	millimetres	mm
ft	feet	0.3048	metres	m
yd	yards	0.914	metres	m
mi	miles	1.61	kilometres	km

### AREA

in <sup>2</sup>	square inches	645.2	millimetres squared	mm <sup>2</sup>
ft <sup>2</sup>	square feet	0.0929	metres squared	m <sup>2</sup>
yd <sup>2</sup>	square yards	0.836	metres squared	m <sup>2</sup>
mi <sup>2</sup>	square miles	2.59	kilometres squared	km <sup>2</sup>
ac	acres	0.395	hectares	ha

### MASS (weight)

oz	ounces	28.35	grams	g
lb	pounds	0.454	kilograms	kg
T	short tons (2000 lb)	0.907	megagrams	Mg

### VOLUME

fl oz	fluid ounces	29.57	millilitres	mL
gal	gallons	3.785	litres	L
ft <sup>3</sup>	cubic feet	0.0328	metres cubed	m <sup>3</sup>
yd <sup>3</sup>	cubic yards	0.0765	metres cubed	m <sup>3</sup>

NOTE: Volumes greater than 1000 L shall be shown in m<sup>3</sup>.

### TEMPERATURE (exact)

°F	Fahrenheit temperature	5/9 (after subtracting 32)	Celsius temperature	°C
----	------------------------	----------------------------	---------------------	----

## APPROXIMATE CONVERSIONS TO SI UNITS

Symbol	When You Know	Multiply By	To Find	Symbol
--------	---------------	-------------	---------	--------

### LENGTH

mm	millimetres	0.039	inches	in
m	metres	3.28	feet	ft
m	metres	1.09	yards	yd
km	kilometres	0.621	miles	mi

### AREA

mm <sup>2</sup>	millimetres squared	0.0016	square inches	in <sup>2</sup>
m <sup>2</sup>	metres squared	10.764	square feet	ft <sup>2</sup>
km <sup>2</sup>	kilometres squared	0.39	square miles	mi <sup>2</sup>
ha	hectares (10 000 m <sup>2</sup> )	2.53	acres	ac

### MASS (weight)

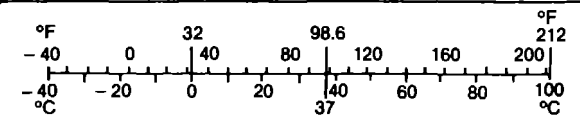
g	grams	0.0353	ounces	oz
kg	kilograms	2.205	pounds	lb
Mg	megagrams (1 000 kg)	1.103	short tons	T

### VOLUME

mL	millilitres	0.034	fluid ounces	fl oz
L	litres	0.264	gallons	gal
m <sup>3</sup>	metres cubed	35.315	cubic feet	ft <sup>3</sup>
m <sup>3</sup>	metres cubed	1.308	cubic yards	yd <sup>3</sup>

### TEMPERATURE (exact)

°C	Celsius temperature	9/5 (then add 32)	Fahrenheit temperature	°F
----	---------------------	-------------------	------------------------	----



These factors conform to the requirement of FHWA Order 5190.1A.

\* SI is the symbol for the International System of Measurements

**CONTENTS**

	Page
Introduction . . . . .	1
Field test sites . . . . .	1
Frost-susceptibility index testing . . . . .	9
Index tests selected . . . . .	10
Laboratory test results . . . . .	12
Conclusions . . . . .	16
Soil column and dual gamma system . . . . .	16
Design features . . . . .	16
Test results . . . . .	18
Mathematical model of frost heave and thaw settlement . . . . .	19
Model development . . . . .	19
Numerical approach . . . . .	22
Probabilistic concepts . . . . .	23
Model verification . . . . .	23
Discussion . . . . .	24
Seasonal variation in the resilient modulus of granular soils . . . . .	25
Characterization by laboratory testing . . . . .	25
Field verification . . . . .	31
Summary of predictive approach . . . . .	36
Simulating frost heave and pavement deflection . . . . .	38
Method of evaluation . . . . .	38
Results and discussion . . . . .	38
Summary of findings . . . . .	40
Frost-susceptibility index tests . . . . .	40
Soil column and dual gamma system . . . . .	40
Mathematical model of frost heave and thaw settlement . . . . .	40
Seasonal variation in resilient modulus of granular soils . . . . .	40
Implementation of research findings . . . . .	41
Corps of Engineers frost design soil classification system . . . . .	41
New laboratory freeze-thaw test . . . . .	41
Frost-heave model . . . . .	41
Repeated-load triaxial test on frozen and thawed soil . . . . .	42
Evaluation of seasonal variation of resilient modulus . . . . .	43
Literature cited . . . . .	43

**ILLUSTRATIONS**

Figure	
1. Winchendon test site . . . . .	2
2. Grain-size distributions of Winchendon test soils and natural subgrade . . . . .	3
3. Ground temperatures prevailing during plate-bearing tests in the Ikalanian sand test section . . . . .	3

Figure	Page
4. Frost depth, heave and moisture tension in the Graves sand test section . . . . .	4
5. Vertical resilient displacement at two load levels and three radii in the Ikalanian sand test section . . . . .	5
6. Test site locations, Albany County Airport . . . . .	6
7. Pavement sections, Taxiways A and B . . . . .	6
8. Grain-size distribution of materials from Taxiways A and B . . . . .	7
9. Freezing isotherms at Taxiway A, 1979-80 . . . . .	7
10. Ground temperatures during plate-bearing tests at Taxiway A, 1982-83 . . . . .	8
11. Moisture tension at Taxiway A, 1979-80 . . . . .	8
12. Vertical resilient displacement at two load levels and three radii, Taxiway B, Test Point T5 . . . . .	9
13. Schematic of new freezing test apparatus . . . . .	11
14. Frost-heave results for the new freeze-thaw test on four samples of Sibley till . .	13
15. Heave rates for all test materials in new freeze-thaw test . . . . .	13
16. CBR values for all test materials in new freeze-thaw test . . . . .	13
17. Comparison of laboratory and field heave rates during first and second freezes .	14
18. Comparison of CBR after thawing with maximum resilient pavement deflection during thawing . . . . .	14
19. Comparison of frost-susceptibility classifications by the methods studied . . . . .	15
20. Soil column . . . . .	16
21. Dual gamma system . . . . .	17
22. Thaw settlement in two soil-column tests on Graves sand . . . . .	18
23. Temperatures and pore pressures in two soil-column tests on Graves sand . . . . .	19
24. Typical model simulation result at a given time . . . . .	21
25. Nonuniform soil profile divided into elements and nodes and showing boundary conditions . . . . .	22
26. Measured and simulated frost depth and frost heave, laboratory soil-column test on Fairbanks silt . . . . .	23
27. Measured and simulated frost depth and frost heave, Taxiway B, Albany County Airport, 1979-80 . . . . .	24
28. Resilient modulus vs unfrozen water content for three frozen Winchendon soils	26
29. Resilient modulus vs temperature for the six Winchendon test soils in the frozen state . . . . .	27
30. Resilient modulus of thawed Hyannis sand vs $J_1$ . . . . .	28
31. Resilient modulus vs $J_2/\tau_{oct}$ for the test data given in Figure 30 . . . . .	28
32. Coefficient $K_1$ of the empirical models vs moisture tension for several soils from Taxiway B, Albany Airport . . . . .	31
33. Deflection basins measured in 1980 FWD test, Hart Brothers sand test section.	32
34. Vertical resilient displacement observed on six test sections prior to freezing, while frozen and during thawing . . . . .	32
35. Measured surface deflections compared with deflections calculated by NELAPAV for three test sections . . . . .	34
36. Measured surface deflections compared with deflections calculated by NELAPAV, 1982-83 . . . . .	35
37. Interpretation of seasonal variation in the resilient modulus of six test soils directly beneath asphalt pavement . . . . .	36
38. Seasonal variation in the resilient modulus of the base and subbase at radius 0.0, Taxiway A, test point C4, 1979-80 . . . . .	37

Figure	Page
39. Seasonal variation in the resilient modulus of the base, subbase and subgrade at radius C.0, Taxiway B, test point T5, high load, 1979-80 and 1980-83 . . . . .	37
40. Comparison of simulated frost heave, frost and thaw depths, and pavement deflection with field observations, Graves sand test section 1978-79 . . . . .	39
41. Implementation of the Corps of Engineers frost design soil classification system	41
42. Implementation of the new freeze test . . . . .	41
43. Implementation of the frost-heave model . . . . .	42
44. Implementation of the repeated-load triaxial test for stress-strain-deflection analysis . . . . .	42
45. Implementation of the seasonally varying resilient modulus for stress-strain-deflection analysis with a cumulative damage approach . . . . .	43

**TABLES**

Table	
1. U.S. Army Corps of Engineers frost design soil classification system . . . . .	10
2. Summary of frost-susceptibility ratings according to all criteria . . . . .	12
3. Preliminary frost-susceptibility criteria for the new freezing test . . . . .	14
4. Results of regression analyses, asphalt concrete and test soils from Winchendon	29
5. Results of regression analyses, asphalt concrete and test soils from Albany Airport . . . . .	30
6. Values of Poisson's ratio used in analysis . . . . .	33





# **Frost Action Predictive Techniques for Roads and Airfields**

## **A Comprehensive Survey of Research Findings**

### **INTRODUCTION**

Six years of intensive research has significantly advanced the state of knowledge and the ability to predict the effects of frost action on pavement performance. The two principal adverse effects of frost are ice segregation, causing heave and transient pavement roughness, and thaw weakening of subgrade and unbound base materials, causing accelerated pavement cracking and pavement deformation (Johnson et al. 1975). In the past, designers of new and rehabilitated pavement projects have necessarily applied thickness design methods that are essentially empirical, reflecting pavement substructure designs that have performed adequately under similar conditions in the past. While the empirical approaches have been quite successful, it has long been an important goal not only to improve them but specifically to develop quantitative methods for predicting the surface heave of a pavement section and for evaluating the seasonal changes in supporting capacity of subgrade and base materials that would affect pavement performance under traffic loads (Johnson et al. 1975).

Having a common interest in these goals, three agencies jointly sponsored the research: the Federal Highway Administration, the Federal Aviation Administration and the U.S. Army Corps of Engineers (DiMillio and Fohs 1980). The research, which spanned the years from late 1978 through 1984, included equipment development, field and laboratory experiments, and development of mathematical models. The investigations focused on four principal study areas:

- Selection and validation of the most effective laboratory index tests to indicate the susceptibility of soils to detrimental frost action.
- Development of a soil column device with provisions for nondestructive monitoring of changes in soil moisture content and density during freezing and thawing.

- Improvement and validation of a mathematical model of frost heave that had been developed earlier, and incorporation of processes that take place during and after thawing.
- Development of laboratory test methods for characterizing seasonal changes in the resilient modulus of a wide variety of granular soils, and validation of these methods by means of in-situ deflection testing of pavements.

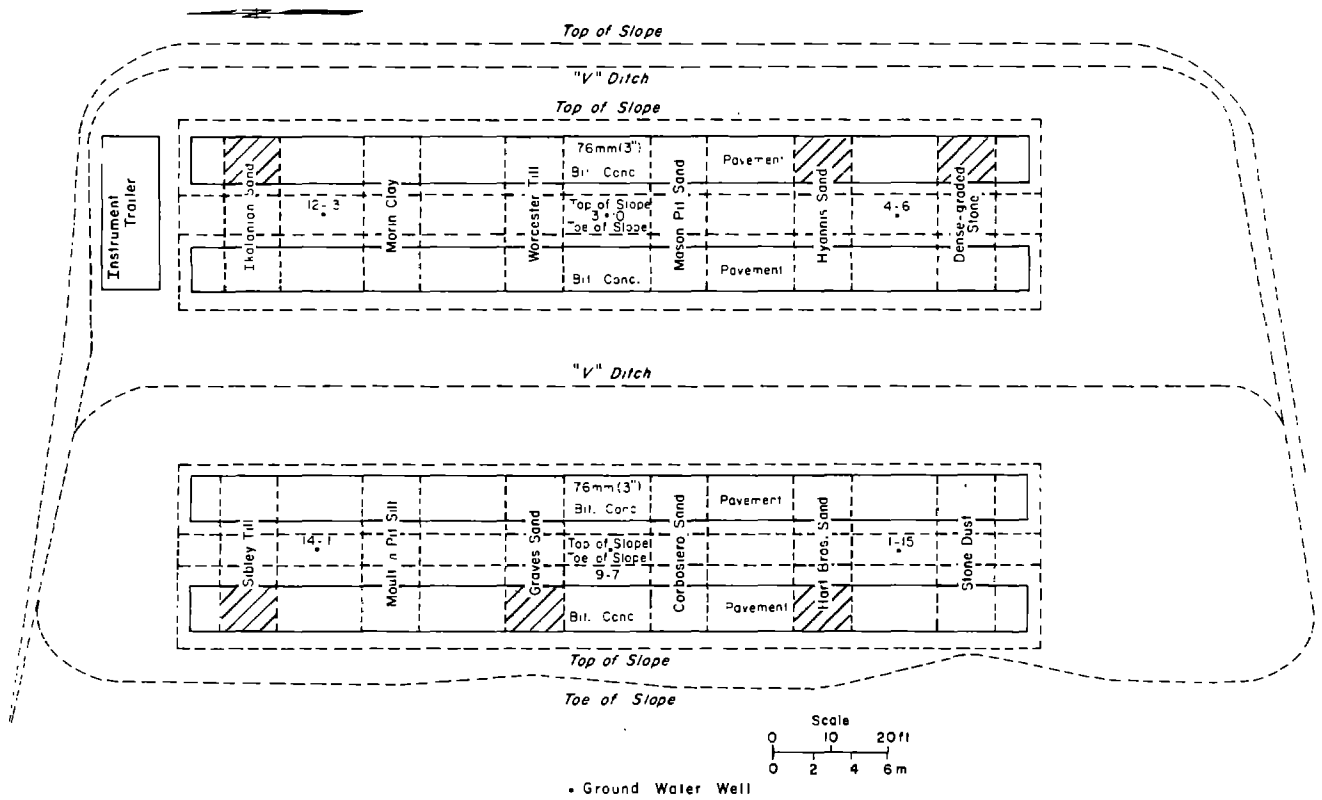
The research also included consideration of means of implementing the findings in pavement design practice, and preparation of flow charts showing how this might be accomplished.

The research was performed by the Army Cold Regions Research and Engineering Laboratory (CRREL). Key investigations were conducted by consultants on certain phases of the work, and we also assembled a board of general consultants who provided guidance and periodic review of the accomplished work. The laboratory testing and analysis were conducted at CRREL's facilities in Hanover, New Hampshire, and field sites at Winchendon, Massachusetts, and Albany County Airport, New York, were used for in-situ testing and data collection.

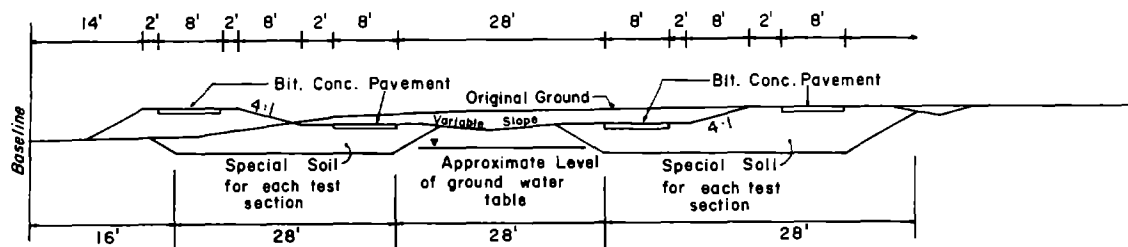
This report presents a comprehensive survey of the research findings in each of the four study areas. Details of the investigations have been documented in one or more research reports on each topic, for which citations are given throughout this report.

### **FIELD TEST SITES**

Field test sites were needed to serve as a source of samples of subgrade soils and base materials for roads and airfield pavements, and as test beds where the performance of these soils and materials in pavement sections could be monitored and test-



a. Plan view.



b. Transverse section.

Figure 1. Winchendon test site.

ed under varied conditions of temperature, moisture and freeze-thaw action and under applied loads. Two sites were used for these purposes.

The first is the Winchendon, Massachusetts, test site, constructed in 1978 by the Massachusetts Department of Public Works (MDPW). The site consists of 24 soil test sections (Fig. 1). Twelve soils are used, each in embankments of two heights. The higher embankments were chosen for the six test sections used in this research. The sections consist of about 50–90 mm of asphalt concrete and 1.5 m of test soil (either Ikalanian sand, Graves sand, Hart Brothers sand, Hyannis sand, dense-graded stone or Sibley till) overlying the natural subgrade, a clean gravelly sand (see grain-size curves, Fig. 2). The water table is about 1.4 m

below the pavement surface. Data were collected from each of the six test sections (Johnson et al. 1986a, Guymon et al., in prep.) during the freeze-thaw-recovery seasons of 1978–79 and 1979–80, including the following:

- Temperature, monitored by thermocouples at the surface, within the asphalt concrete, and at various depths in the subgrade (Fig. 3).
- Depth of frost, monitored by thermocouples and by frost tubes previously installed by MDPW (Fig. 4).
- Depth to the water table, monitored in observation wells previously installed by MDPW.
- State of stress in soil moisture, monitored

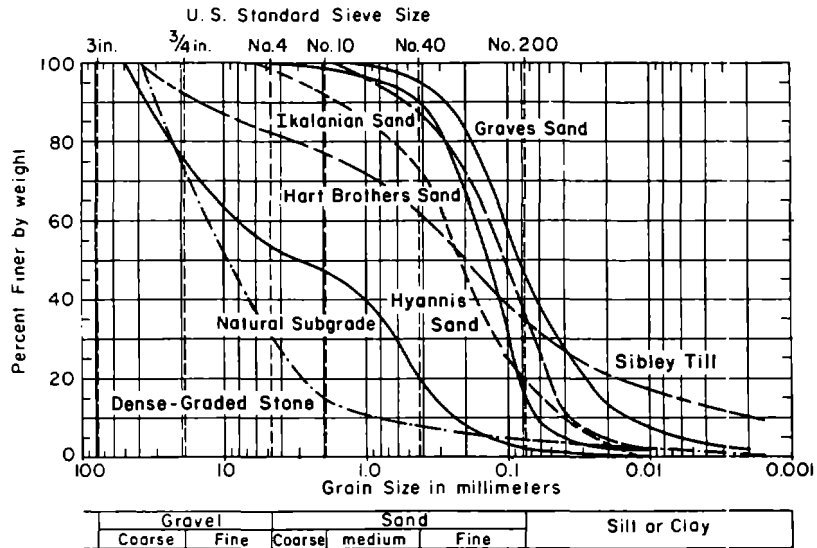


Figure 2. Grain-size distributions of Winchendon test soils and natural subgrade.

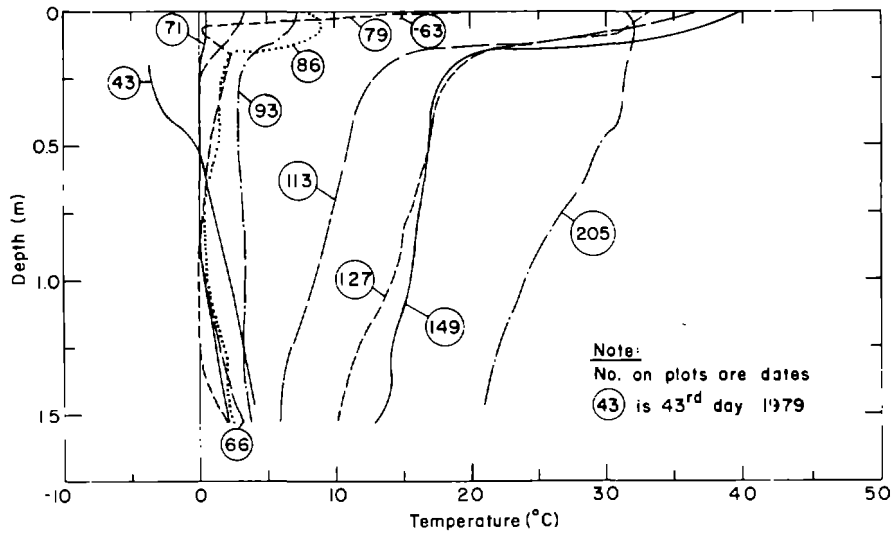


Figure 3. Ground temperatures prevailing during plate-bearing tests in the Ikalanian sand test section.

by means of moisture tensiometers installed in the subgrade at depths of 152, 305, 610 and 914 mm below the paved surface (Fig. 4).

- Vertical displacement of the paved surface under load, measured on the paved surface at a central point on each of the six sections on 13 occasions by repeated-load plate-bearing (RPB) tests and by falling-weight deflectometer (FWD) tests on nine occasions (Fig. 5).
- Vertical displacement of the paved surface caused by freezing and thawing, measured

by level surveys conducted by MDPW (Fig. 4).

- Meteorological data, including precipitation and air temperature, monitored by means of a precipitation gauge and a thermograph.

The second test site is at Albany County Airport, located 10 km north of Albany, New York, where two pavements were selected for field testing: Taxiways A and B (Fig. 6). Taxiway A is a new pavement that was under construction in 1979 when we installed the instrumentation, and the first loading tests were performed prior to any air-

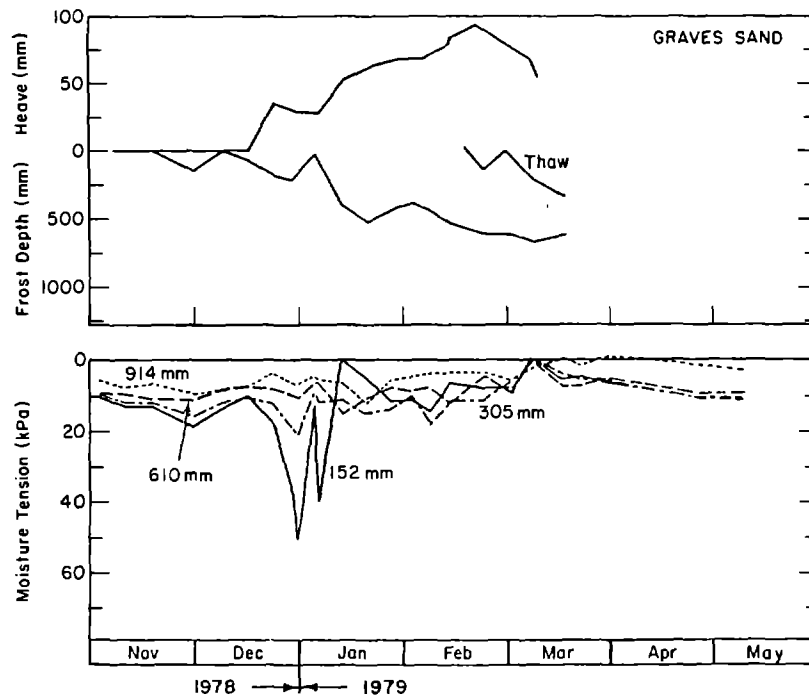


Figure 4. Frost depth, heave and moisture tension in the Graves sand test section.

craft traffic. The pavement cross section (Fig. 7) consists of 330 mm of asphalt concrete, 584 mm of crushed stone base and 914 mm of gravelly sand subbase over a subgrade of silty fine sand. The grain-size distribution curves (Fig. 8) show that both the base and subbase materials have significant fine fractions, with about 12% passing the No. 200 sieve and about 9% finer than 0.02 mm. In both cases the fines are nonplastic.

Taxiway B, constructed many years ago (possibly in the 1940s), is no longer used as a taxiway and is used only occasionally for parking light aircraft. The surface is uneven and the asphalt concrete is aged and severely cracked. The asphalt concrete is 76 mm thick and overlies about 102 mm of asphalt-penetration macadam stone base and 127 mm of gravel subbase (Fig. 7). The subgrade is silty fine sand. The penetration macadam base is aged and deteriorated to the point of being quite friable and is not clearly distinguishable from the subbase. Consequently the samples of the subbase whose composite grain-size distribution is shown in Figure 8 were taken to represent a single 229-mm base-subbase layer.

Boring records showed groundwater about 2.3 m below the pavement of Taxiway A and 1.8 m at Taxiway B. We installed groundwater observation wells at both taxiways and found that the depth

fluctuates seasonally between about 1.5 and 2.0 m at both sites.

The following data were collected at each of the test pavements at Albany County Airport (Guymon et al., in prep., Johnson et al. 1986b) during the four freeze-thaw-recovery seasons from 1979 to 1983, except as noted:

- Temperature, monitored by thermistors at the surface, within the asphalt concrete, and at various depths in the base, subbase and subgrade (Fig. 10).
- Depth to the water table, monitored in observation wells adjacent to the taxiways.
- State of stress in soil moisture, monitored by tensiometers at depths of about 533, 813, 1118 and 1524 mm below the pavement surface at Taxiway A and 480, 640, 840 and 1140 mm below the pavement surface at Taxiway B (Fig. 11).
- Vertical displacement of the pavement surface under load, measured by the RPB device on two occasions and by the FWD device on 10 occasions in the 1979-80 season, and 11 times by the FWD device in 1982-83 (Fig. 12).
- Vertical displacement of the pavement surface due to freezing and thawing, measured by rod and laser level surveys.

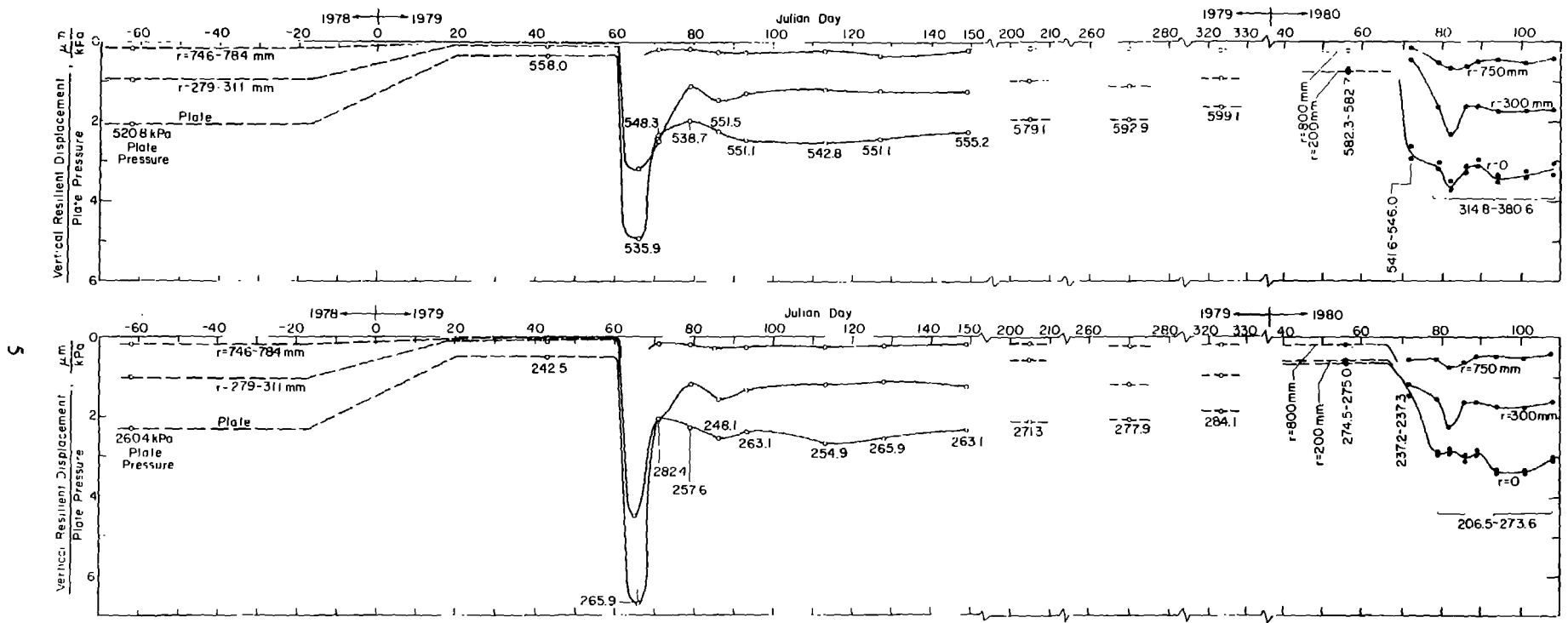


Figure 5. Vertical resilient displacement at two load levels and three radii in the Ikalanian sand test section (RPB tests in 1978-79 and FWD tests in 1980).

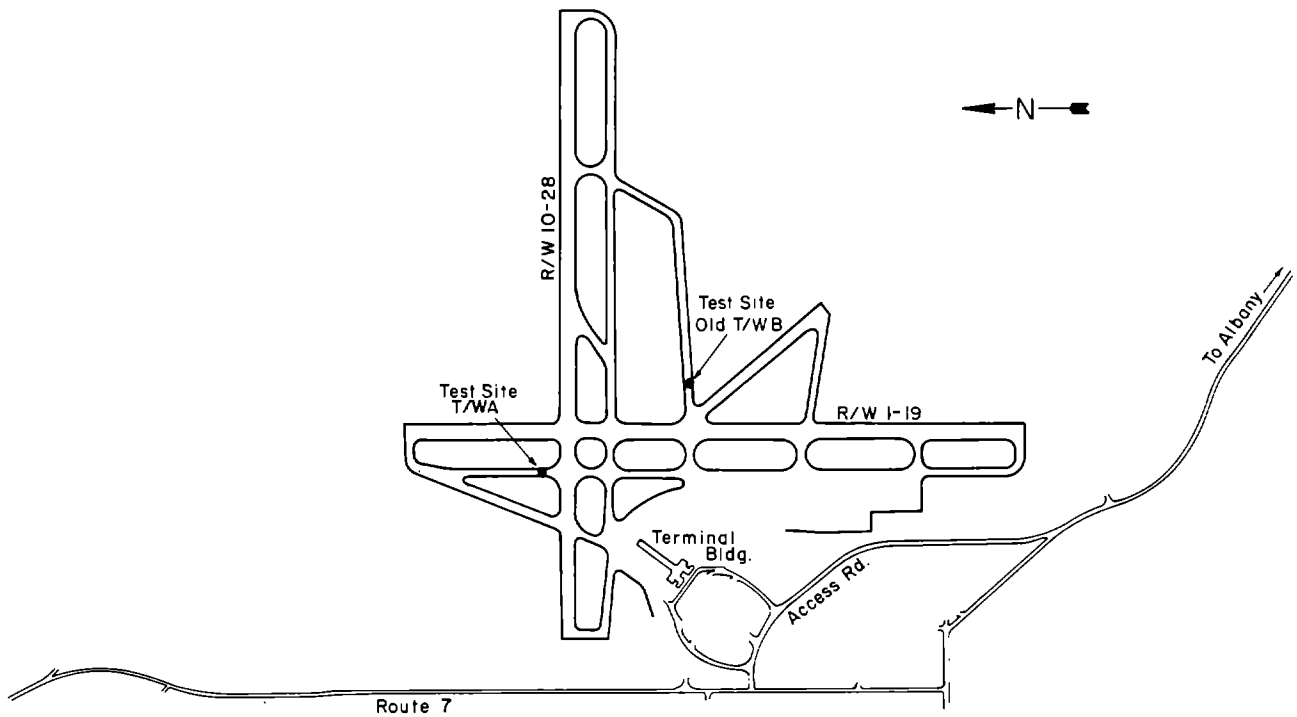


Figure 6. Test site locations, Albany County Airport, Albany, New York.

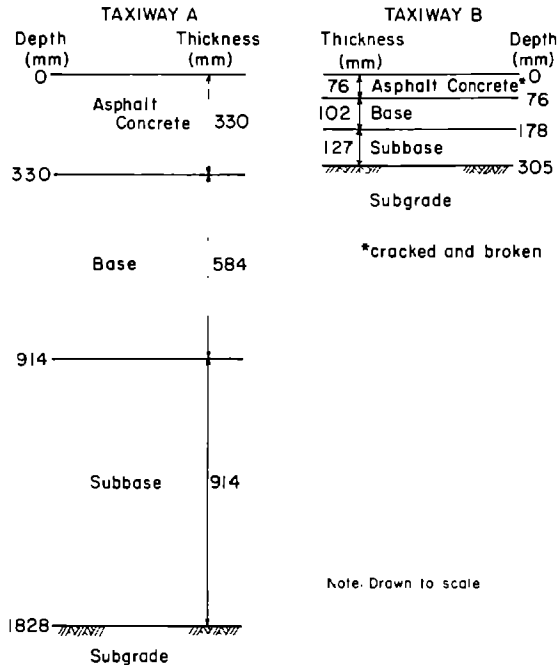


Figure 7. Pavement sections, Taxiways A and B.

- Meteorological data, including precipitation, wind speed and direction, and air temperature, obtained from the National Weather Service station at the airport.

In addition to the data collection and in-situ testing at the Winchendon and Albany County Airport sites, we also used samples from the same test sections for related laboratory tests. Core samples of the asphalt concrete, 102 mm in diameter, were taken, and 57-mm-diameter undisturbed samples of the finer soils were obtained in the fall prior to freeze-up. Once frost had advanced to sufficient depth in the sections, core samples of the frozen soil were taken, except those materials containing numerous gravel-size fragments. Bulk samples of about 40-50 kg also were obtained from each soil and base material.

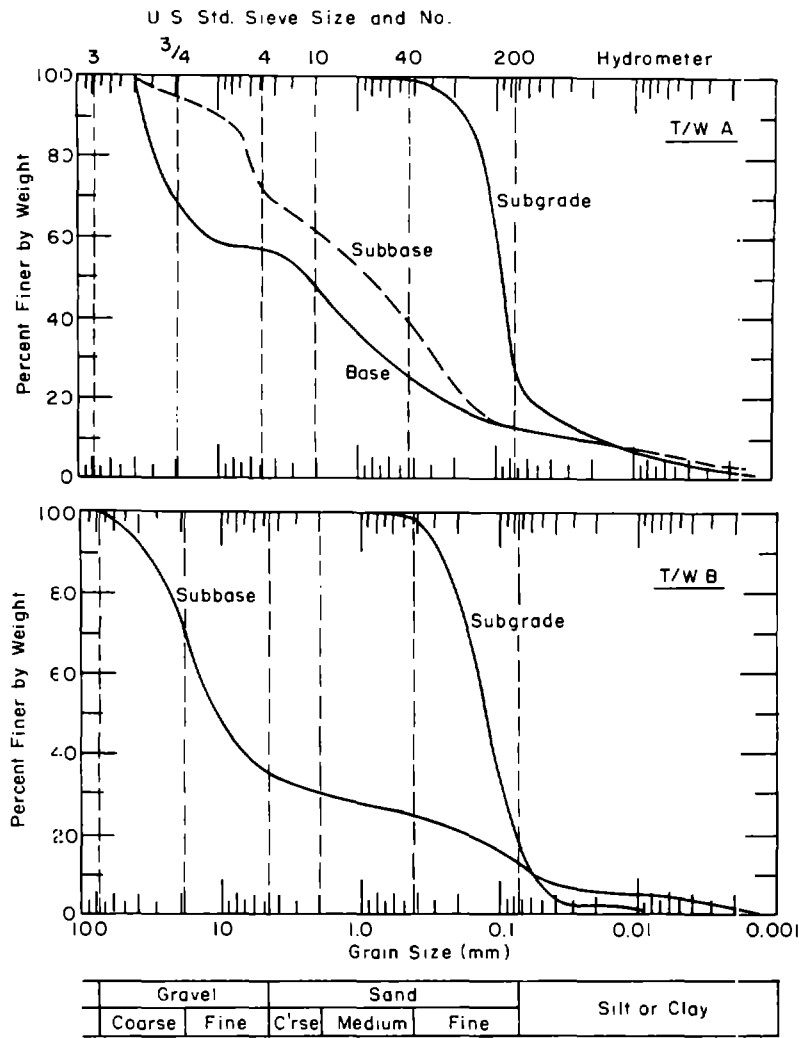


Figure 8. Grain-size distribution of materials from Taxiways A and B.

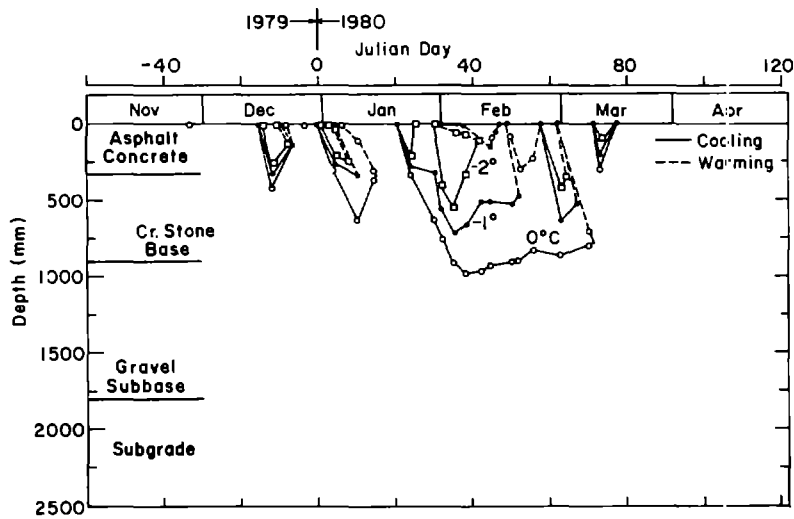


Figure 9. Freezing isotherms at Taxiway A, 1979-80.

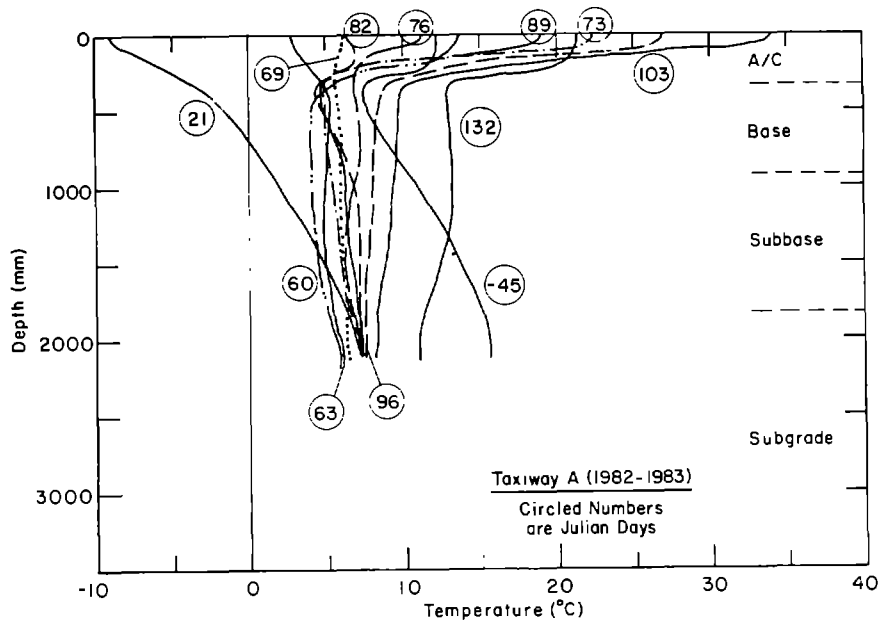


Figure 10. Ground temperatures during plate-bearing tests at Taxiway A, 1982-83.

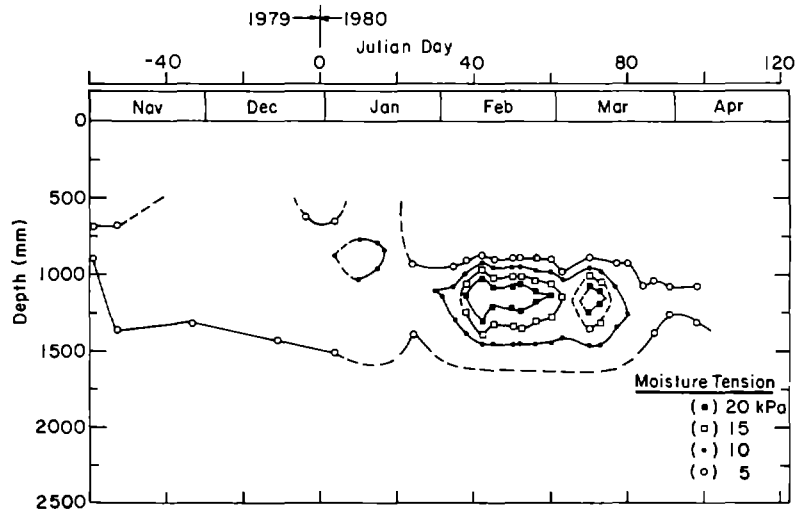


Figure 11. Moisture tension at Taxiway A, 1979-80.



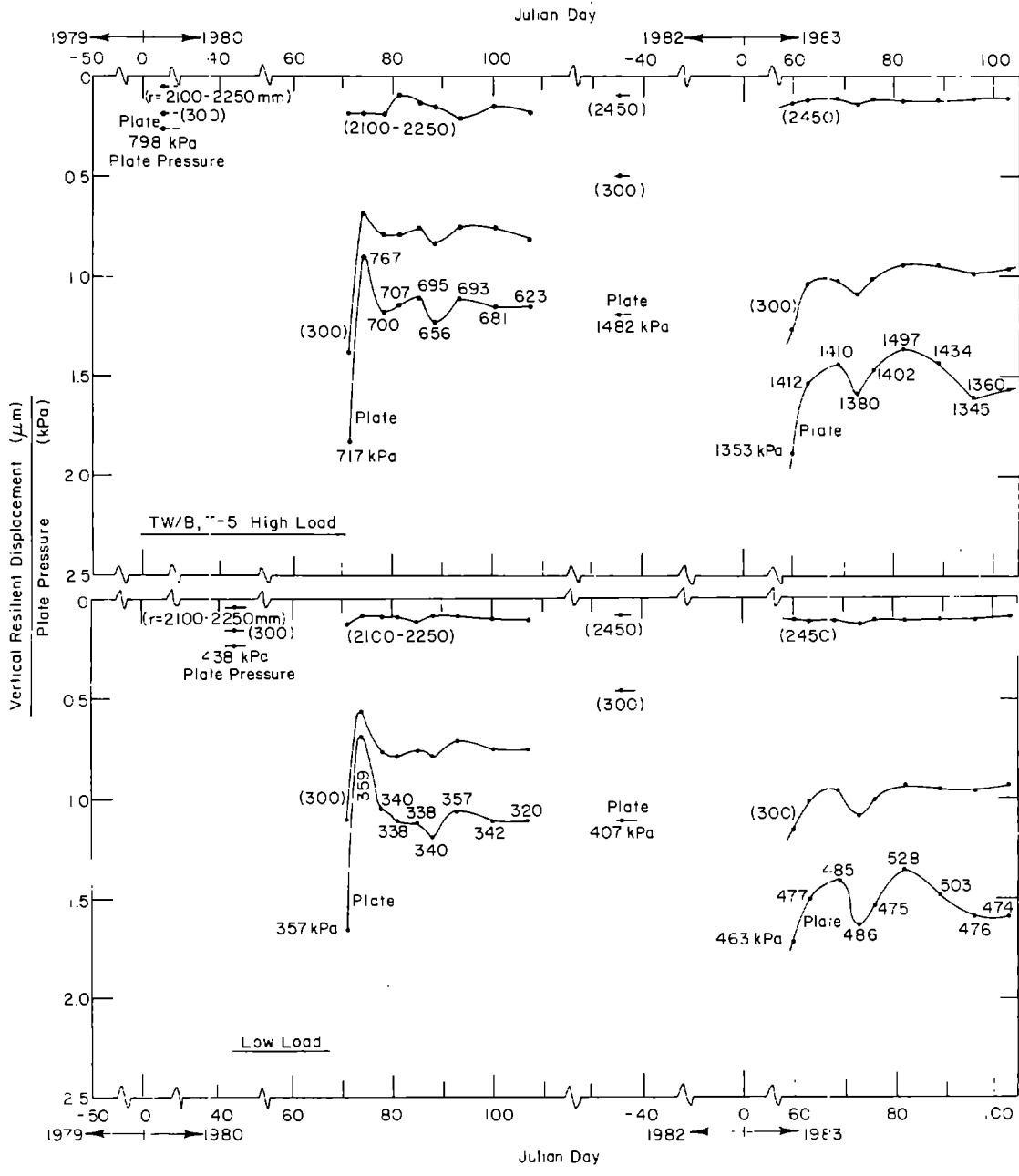


Figure 12. Vertical resilient displacement at two load levels and three radii, Taxiway B, Test Point T5.

**FROST-SUSCEPTIBILITY INDEX TESTING**

Frost-susceptibility index tests allow geotechnical engineers to determine the potential for frost heaving and thaw weakening of subgrade soils and unbound base and subbase materials in roads and airfields. In a survey of transportation departments throughout the world, Chamberlain et al. (1984) found that most agencies have developed

their own unique frost-susceptibility index criteria based on laboratory tests, that these criteria fail to discriminate marginally frost-susceptible material from material that is frost susceptible, and that there is little documentation of the efficacy of the adopted standards. Furthermore, most of the various tests consider only frost heave or thaw weakening rather than both, and most of those that employ laboratory freezing tests require excessive time and impose poor control of test conditions.

The objective of this study was to develop improved index test methods for fully characterizing the frost susceptibility of soils. To accomplish this task, a thorough review of frost-susceptibility index tests and practices of transportation agencies was made. The index tests were categorized into three types or levels of complexity. The efficacy of each test was identified and the attributes and deficiencies were noted.

During the evaluation phase it was decided that one index test from each of the three types would be selected for further evaluation. This was done so that a geotechnical engineer could select an index test with a particular level of reliability and complexity commensurate with the size and scope of a project.

The index tests selected include the U.S. Army Corps of Engineers frost design soil classification system, a moisture-tension/hydraulic-conductivity test, and a new freezing test containing both frost-heave and thaw-weakening elements. These

tests were run on the materials from the Winchendon and Albany test sites. The results were compared with field observations of frost heave and thaw weakening at the test sites, and the validity of each test was determined.

Details of the selection process, the procedures for the selected tests, and the analysis of the data are given in three reports by Chamberlain (1981a, 1981b, in prep. a).

### Index tests selected

#### *Corps of Engineers method*

The U.S. Army Corps of Engineers frost design soil classification system (Berg and Johnson 1983) in its present form is shown in Table 1. It is based on three levels of screening: (level I) the percentage of particles smaller than 0.02 mm, (level II) the soil type under the Unified Soil Classification System, and (level III) a laboratory freezing test. The ratings of frost-susceptible soils according to

**Table 1. U.S. Army Corps of Engineers frost design soil classification system.**

<i>Frost susceptibility*</i>	<i>Frost group</i>	<i>Kind of soil</i>	<i>Amount finer than 0.02 mm (% by weight)</i>	<i>Typical soil type under Unified Soil Classification System†</i>
Negligible to low	NFS**	a) Gravels	0-1.5	GW, GP
		b) Sands	0-3	SW, SP
Possibly	PFS††	a) Gravels	1.5-3	GW, GP
		b) Sands	3-10	SW, SP
Low to medium	S1	Gravels	3-6	GW, GP, GW-GM, GP-GM
Very low to high	S2	Sands	3-6	SW, SP, SW-SM, SP-SM
Very low to high	F1	Gravels	6-10	GM, GW-GM, GP-GM
Medium to high	F2	a) Gravels	10-20	GM, GM-GC, GW-GM, GP-GM
		b) Sands	6-15	SM, SW-SM, SP-SM
Medium to high	F3	a) Gravels	> 20	GM, GC
Low to high		b) Sands except very fine silty sands	> 15	SM, SC
Very low to very high		c) Clays, PI > 12	—	CL, CH
Low to very high	F4	a) All silts	—	ML, MH
		b) Very fine silty sands	> 15	SM
Low to very high		c) Clays, PI < 12	—	CL, CL-ML
Very low to very high		d) Varved clays and other fine-grained, banded sediments	—	CL and ML; CL, ML and SM; CL, CH, and ML; CL, CH, ML and SM

\* Based on laboratory frost heave-tests.

† G—gravel, S—sand, M—silt, C—clay, W—well graded, P—poorly graded, H—high plasticity, L—low plasticity.

\*\* Non-frost-susceptible.

†† Requires laboratory frost-heave test to determine frost susceptibility.

this method are given in six categories: negligible, very low, low, medium, high and very high. The simplest rating (based on level I tests) is the classification of negligible frost susceptibility given to gravels with less than 1.5% finer than 0.02 mm and sands with less than 3% finer than 0.02 mm. Any soil failing this criterion requires complete soil classification tests (level II). Gravels with 1.5–3% finer than 0.02 mm and sands with 3–10% finer than 0.02 mm also require a laboratory frost-heave test (level III). The range of possible degrees of frost susceptibility is very wide for most soils. For this reason, the Corps of Engineers procedure includes the recommendation that a freezing test be performed for more precise determination of the degree of frost susceptibility of all frost-susceptible soils.

*Moisture-tension/  
hydraulic-conductivity test*

The second laboratory test selected for consideration was a moisture-tension/hydraulic-conductivity test. This test was selected because it addresses the fundamental causes of ice segregation and frost heave more directly than particle-size tests do. It is also a test that is routinely conducted at CRREL for research purposes and was already included in the frost-heave modeling part of this research project. However, the lengthy period of time required to conduct this test, the requirement for a very skillful technician, and the inconclusive nature of the results led to the conclusion that this test is not suitable for determining the frost susceptibility of soils. Details of this evaluation are given by Chamberlain (in prep. a).

*New freezing test*

As a result of the literature review, it was concluded that all available freezing tests have at least one serious fault. The flaws include too small or too large a sample size, significant radial heat flow, lack of surcharge, insufficient control of moisture availability, lack of appropriate frost-susceptibility assessment criteria, and insufficient field validation. Our experience with the CRREL freezing test (Kaplar 1974, Chamberlain and Carbee 1981) specified as part of the Corps of Engineers procedures for pavement design in frost areas (Berg and Johnson 1983) indicates that it suffers from several defects. The most significant are poor temperature control, indeterminate side friction, lengthy test period, lack of thaw weakening index, and provision for only a single freeze.

It was concluded that a new freezing test should

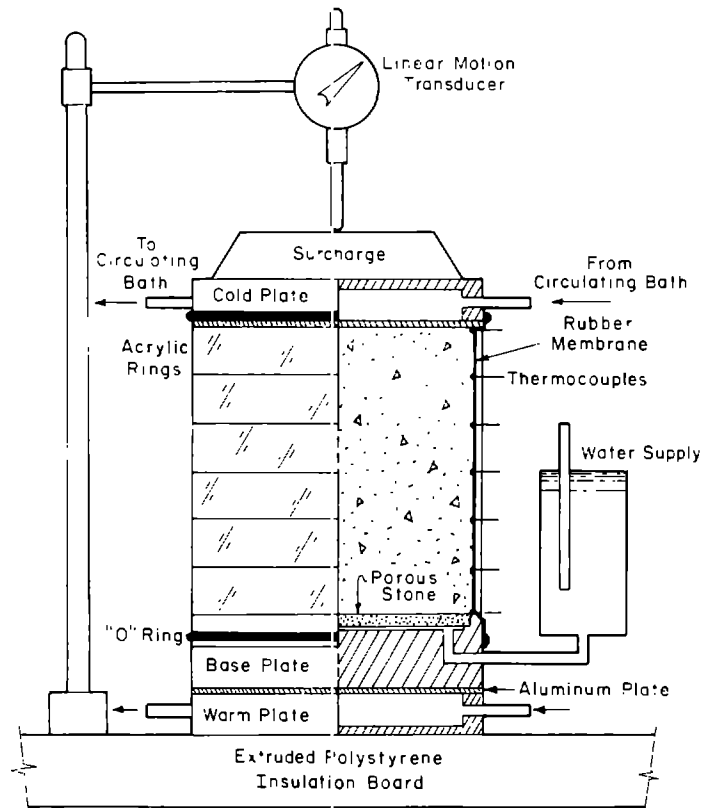


Figure 13. Schematic of new freezing test apparatus.

be developed, for which we established the following basic guidelines:

- The test should be as simple as possible, so that highway and geotechnical laboratories can conduct tests readily.
- The results must be reliable.
- The test conditions must bear a relation to freezing conditions in the field.
- The test conditions must also relate to thaw weakening in the field.
- The test must be of short duration.
- The test must accommodate the complete range of material types from granular base and subbase materials to fine-grained subgrade materials.
- The apparatus should be inexpensive to construct and operate.

We developed a new freezing test using these guidelines (Fig. 13). The equipment includes a rubber-membrane-lined, multi-ring freezing cell to minimize side friction, liquid-cooled cold plates for precise top and bottom boundary temperature control, and a data acquisition and control system for automated temperature control and data processing. The test imposes two freeze-thaw cycles to account for the changes in susceptibility to frost

heave caused by a prior freeze-thaw cycle. Four samples are tested, each 150 mm in diameter and 150 mm in height. Samples of prepared material are compacted to field density and moisture conditions. Water is freely available through porous base plates. The test requires five days to complete. The heave rate at the end of the first eight hours of each two-day freeze-thaw cycle is used as an index of frost-heave susceptibility. A CBR test is conducted after the second thaw to provide an index of thaw-weakening susceptibility. As will be seen, both indices (frost heave and thaw weakening) must be used to determine the frost susceptibility of a soil. Details of the test and the procedures are provided by Chamberlain (in prep. b).

#### Laboratory test results

Particle-size tests, Atterberg-limit tests, and the new freezing test were performed on the materials from the Winchendon and Albany test sites.

#### Corps of Engineers method

Frost-susceptibility ratings according to the Corps of Engineers frost design soil classification method are shown in Table 2. All but one of the soils (Hyannis sand) were rated frost susceptible by this method. The frost-susceptibility ratings vary widely and do not appear to be strongly related to either the heave rate or the pavement deflection observed in the field. The rating correctly identifies the Hyannis sand as non-frost-susceptible (negligible to low frost susceptibility) in terms of the frost heave measured in the field, but the other soils require freezing tests to determine their degree of frost susceptibility.

The frost susceptibilities of the test soils were also determined (Table 2) by finding a similar soil in a table of previous CRREL freezing test results published by Kaplar (1974) and as part of Corps of Engineers guidance on this subject (Berg and Johnson 1983). The Hyannis sand was the only test soil that received a rating of non-frost-susceptible. Others, such as the dense-graded stone and Graves sand, are ranked highly frost susceptible. Most notable is the considerably narrower range of frost susceptibility for each soil given by this method than that obtained by the particle-size and soil classification method.

The frost susceptibilities of the test soils were also determined from the CRREL standard freezing test in the tapered cylinder. Table 2 also summarizes the test results. Again, the Hyannis sand was ranked as the lowest in frost susceptibility among the Winchendon materials. The lowest rating of all the test materials, however, was for the Albany Airport Taxiway B subgrade material

#### New freezing test

An example of the results of the new freezing test is shown in Figure 14. Four freezing tests were conducted on each of the Winchendon soils and two on each of the Albany materials. The heave rates (Fig. 15) were lowest for Hyannis sand and highest for the Sibley till material. The high heave rates for Sibley till material occurred during the second freeze. Sibley till also had the lowest CBR values after the second thaw (Fig. 16). The Taxiway B subgrade material had the highest post-thaw CBR.

Figure 15 shows that the frost-heave rates for

**Table 2. Summary of frost-susceptibility ratings according to all criteria.**

	Existing methods			New freezing test		CBR after thawing	Range of field observations	
	Corps of Engineers grain size classification	Comparison with tabulated data	CRREL freezing test	(8-hr heave rate) 1st freeze    2nd freeze			Heave rate	Pavement deflection
<b>Winchendon</b>								
Dense-graded stone	VL-H	H	M	M	M	M	VL-M	M
Graves sand	L-H	H	H	H	M	VH	L-H	H-VH
Hart Brothers sand	VL-H	L	H	M	M	H	VL-M	H
Hyannis sand	N	N	L	VL	VL	M	N-L	M
Ikalanian sand	VL-H	L	M	M	M	H	VL-M	H-VH
Sibley till	VL-H	L-M	L-M	VL	VH	VH	N-VL	H-VH
<b>Albany</b>								
Taxiway A base	N-H	M-H	M	M	H	L	N	N
Taxiway B subbase	VL-H	L-M	H	M	H	M	L	H
Taxiway B subgrade	N-H	L	VL	H	H	VL	L	H

VH—very high; H—high; M—medium; L—low; VL—very low; N—negligible.

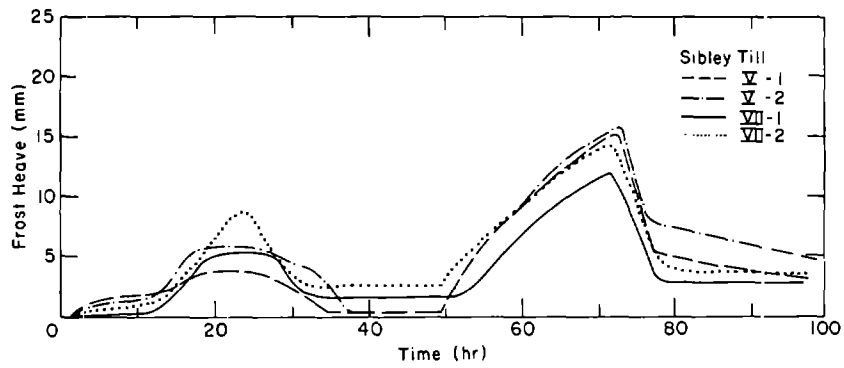


Figure 14. Frost-heave results for the new freeze-thaw test on four samples of Sibley till.

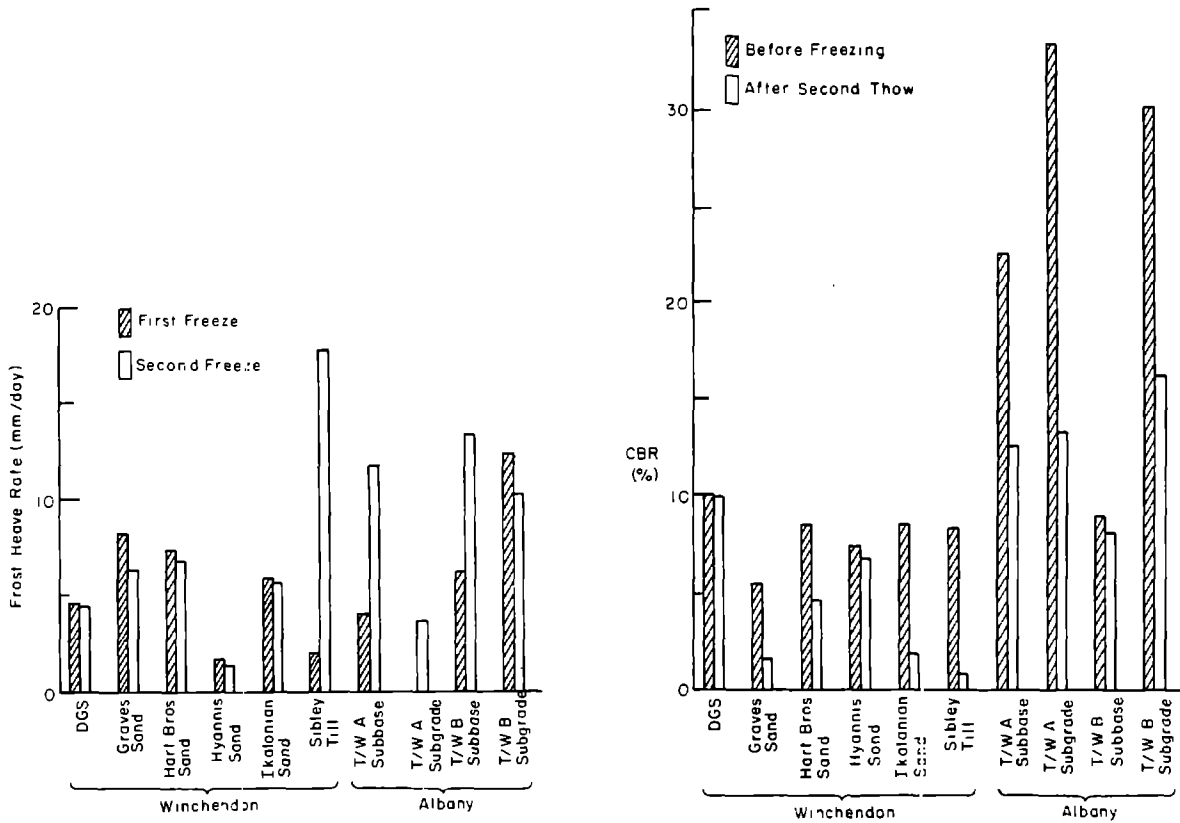


Figure 15. Heave rates for all test materials in new freeze-thaw test.

Figure 16. CBR values for all test materials in new freeze-thaw test.

three of the soils were significantly greater during the second freeze. For two of the soils (Taxiway A base and Taxiway B subbase) the heave rate increased by factors of 2 to 3, while for Sibley till it increased by a factor of 9 from one of the lowest heave rates (2 mm/day) to the highest (18 mm/day). This illustrates the importance of including the second freeze-thaw cycle in this test.

Figure 16 shows that the CBR values were re-

duced by two cycles of freezing and thawing. Again, the detrimental change was greatest for Sibley till, with the CBR being reduced to about 12% of the value before freezing.

#### Discussion

Comparisons of the laboratory and field frost-heave rates are shown in Figure 17. With the exception of the Taxiway A results, there is a strong

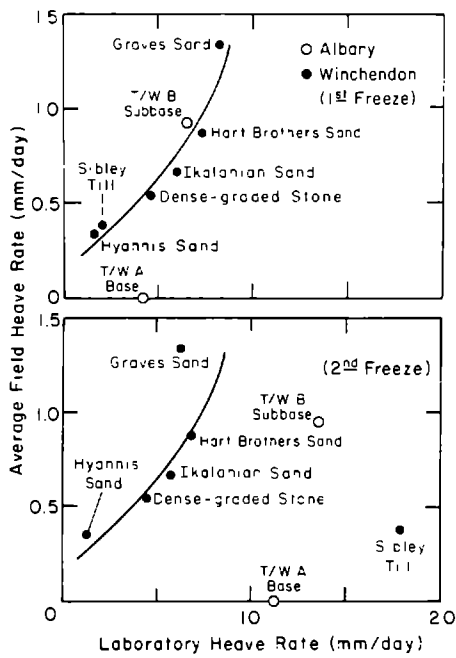


Figure 17. Comparison of laboratory and field heave rates during first and second freezes.

correlation between these heave rates for the first freeze-thaw cycle. The correlation is not on a line of equality, as the laboratory heave rates exceed the field values by a factor of 10 or more. However, since it was the intent of this study to use the freezing test qualitatively, not as a quantitative predictor of frost heave in the field, the differences are not considered significant. When the results are plotted for the second freeze, the correlation between the laboratory and field results becomes weaker, as the points for the two Albany base materials and the Sibley till fall far to the right of the curve fitting the remainder of the data.

The correlation between the CBR after thawing and the maximum resilient pavement deflection during thawing (Fig. 18) is better than the correlation between the frost-heave parameters. In this case, all the average values of deflection fall close to a straight line showing inverse proportionality with CBR after thawing.

The comparisons in Figures 17 and 18 clearly show the need for including a thaw-weakening indicator as a frost-susceptibility index in the laboratory freezing test. If only the heave rate from the first freeze had been used to determine the frost susceptibility of the Sibley till, the soil would have been called non-frost-susceptible. The results of the second freeze, the CBR after thawing, and the

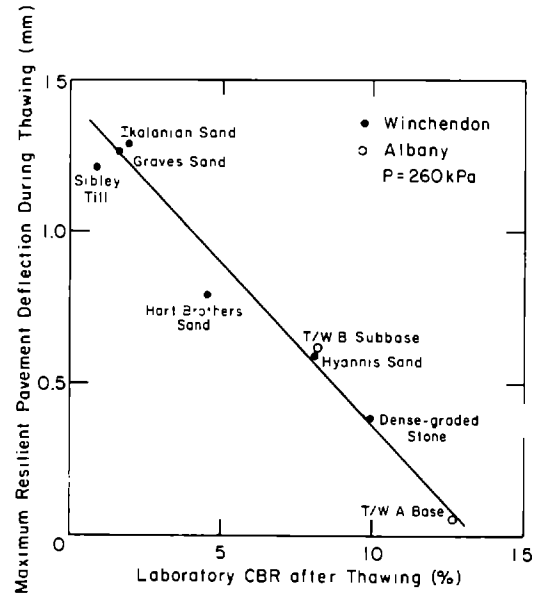


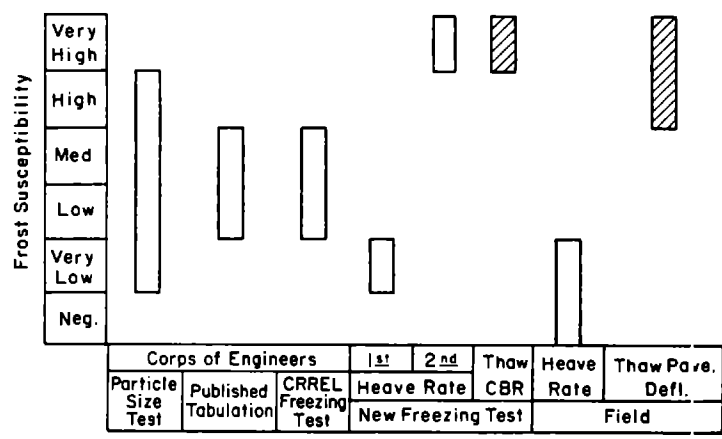
Figure 18. Comparison of CBR after thawing with maximum resilient pavement deflection during thawing.

pavement deflection under load in the field show that this soil is clearly frost susceptible.

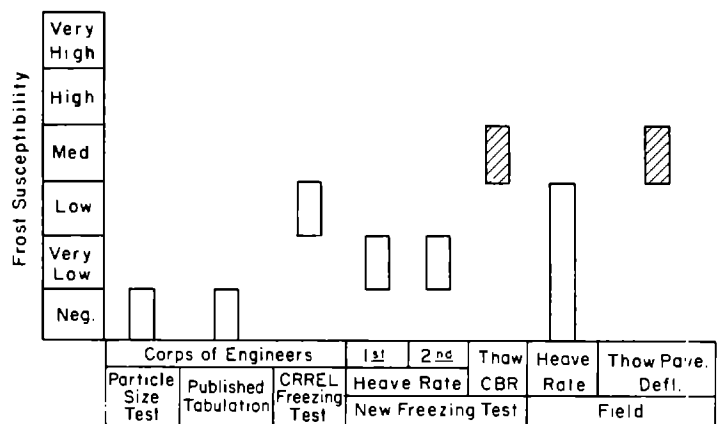
As it was desirable to compare at least qualitatively the results of the various test methods for the test soils, preliminary frost-susceptibility classification criteria were established for the new freezing test. These criteria are shown in Table 3. They are based on the average frost-heave rate during the first 8 hours of the first freeze and the CBR after two cycles of freezing and thawing. The criteria were established by comparing a limited number of laboratory and field tests, so they must be considered preliminary and subject to change.

Table 3. Preliminary frost-susceptibility criteria for the new freezing test.

Frost-susceptibility classification	Heave rate (mm/day)	Thaw CBR (%)
Negligible	< 1	> 20
Very low	1-2	20-15
Low	2-4	15-10
Medium	4-8	10-5
High	8-16	5-2
Very high	> 16	< 2



a. Sibley till.



b. Hyannis sand.

Figure 19. Comparison of frost-susceptibility classifications by the methods studied.

Frost-susceptibility criteria for the field observations were also developed for comparison with the criteria for the new test. Details of these ratings are given by Chamberlain (in prep. a). Table 2 shows ratings of all the test materials using the criteria for the new freezing tests and the field observations along with a summary of the ratings using the other procedures in this study. The bar charts in Figure 19 illustrate the range of frost-susceptibility classifications for two of the test soils.

The comparisons of the laboratory results and the field observations show that the Corps of Engineers particle-size test was effective in rating non-frost-susceptible soils but was not effective in determining the degree of frost susceptibility of the other soils. Estimates made from published results of previous CRREL freezing tests predict frost-heaving behavior better. However, it is clear from the test results for several of the study materials, and especially for the Sibley till results, that a

thaw-weakening indicator such as the CBR test after freezing and thawing is required.

The importance of conducting two freeze-thaw cycles is not clearly demonstrated in these tests except by the fact that a prior freeze-thaw cycle can have a dramatic effect on the behavior during freezing in the laboratory. The heave rates during the second freeze probably correlate poorly with the field heave rates because prior freeze-thaw cycles at the field sites had not extended through the full depth of the test material to the water table. The entire path through which water must flow from the water table to the frost front was not preconditioned by prior freezing and thawing as it was in the laboratory. Thus, laboratory frost-susceptibility ratings obtained from a second freeze are probably useful only when prior frost cycling in the field fully penetrates the material to the water table. More field experience is needed to fully understand this problem.

## Conclusions

It is clear from this study that to determine the frost susceptibility of a soil accurately, it is necessary to conduct a freezing test. While the Corps of Engineers frost design soil classification method is useful for separating non-frost-susceptible soils from frost-susceptible soils, it is not very helpful in determining their degree of frost susceptibility, and it cannot be effectively used to predict the degree of thaw-weakening susceptibility.

The heave rate in the laboratory freezing test can be used to determine the frost-heave susceptibility in the field, and the CBR value after freezing and thawing is a strong indicator of field thaw weakening leading to increased resilient pavement deflection under load.

The requirement for two freeze-thaw cycles was not clearly demonstrated in these tests; however, it remains a candidate element of the freezing test for use in regions where freeze-thaw cycling actively conditions the soil fabric throughout the full depth to the ground water table.

The freezing test proposed is a feasible candidate for replacing the CRREL freezing test as the standard for the Corps of Engineers because it requires much less time to conduct (5 vs 14 days), it provides much better boundary temperature control, it eliminates the side friction problem prevalent in the current standard test, it provides an indicator of thaw-weakening susceptibility as well as an indicator of frost-heaving susceptibility, and it allows the effects of repeated freezing and thawing to be determined.

As further research using the new freezing test appears justified, the automated equipment necessary to conduct the test should be provided to several transportation laboratories to obtain a larger data base from which more reliable frost-susceptibility criteria can be established. The Corps of Engineers frost design soil classification method based on grain size and soil classification should be included in any additional studies, and the corresponding criteria should be refined based on the experience obtained.

## SOIL COLUMN AND DUAL GAMMA SYSTEM

### Design features

It has long been known that moisture content and soil density change significantly when soil freezes. Changes in these variables, in time and space, need to be evaluated, as they are critical pa-

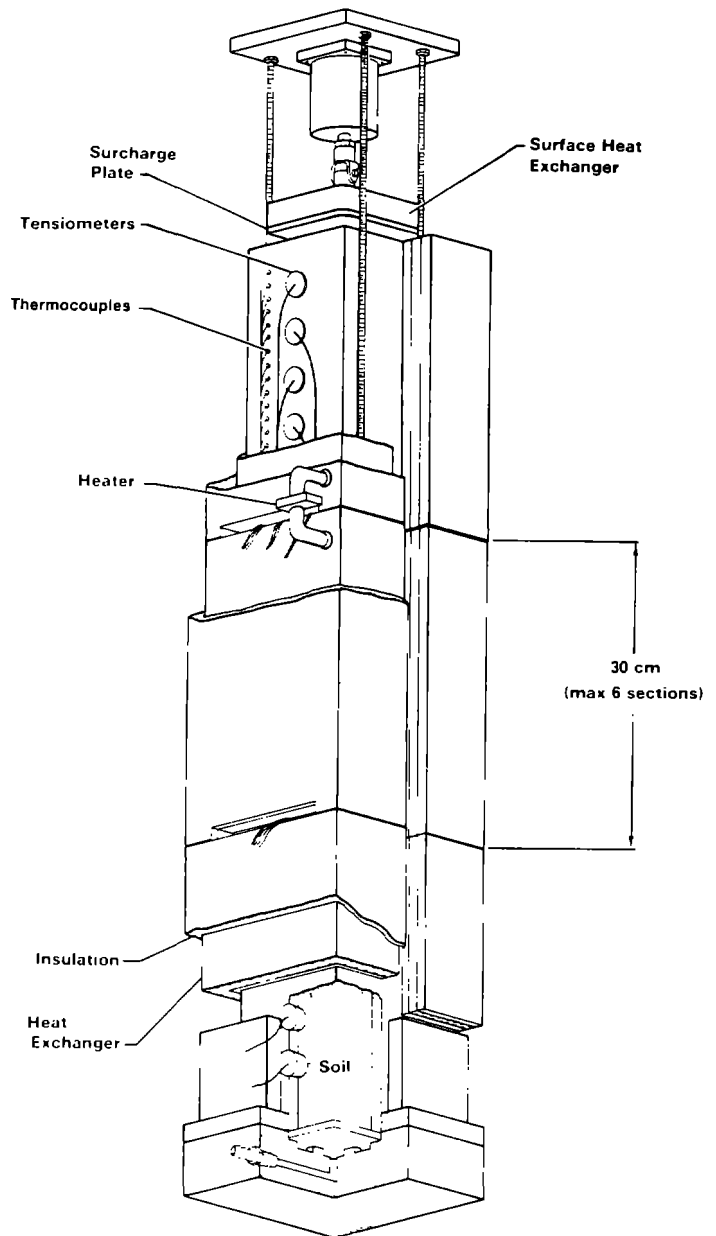


Figure 20. Soil column (schematic).

rameters in heat and mass transfer during freezing and thawing. The soil column and dual gamma system were constructed to generate such data from laboratory tests. The data were then used to develop, verify and refine the mathematical model of frost heave and thaw settlement.

Three separate soil columns were designed and fabricated for this study. The interior dimensions are about 50 mm in diameter, 135 mm in diameter, and 100 mm by 100 mm square, respectively. Figure 20 is a schematic drawing of the square soil column. The columns consist of 300-mm-long seg-



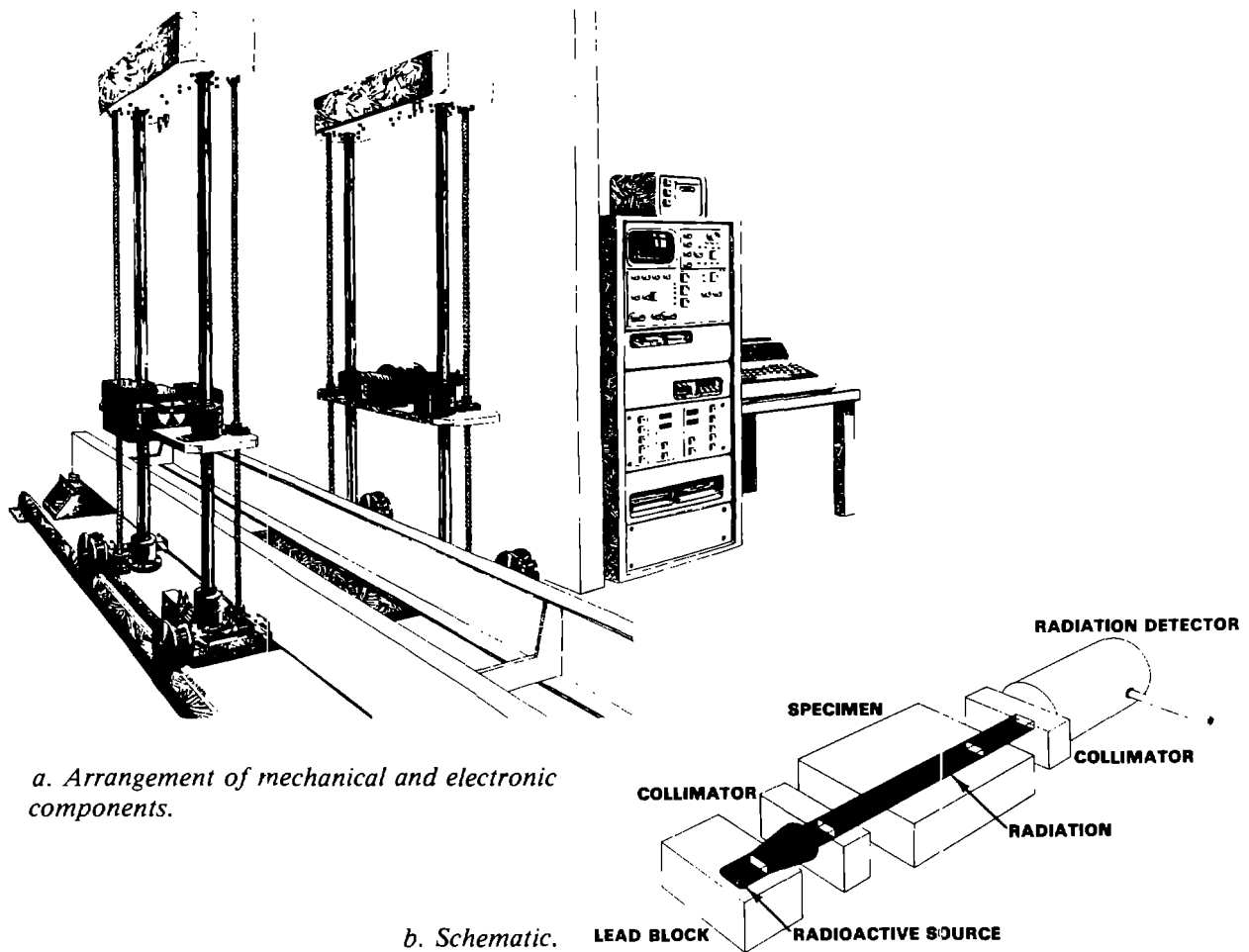


Figure 21. Dual gamma system.

ments that are stacked to provide any desired length from 900 to 1800 mm. The upper 300 mm of the column is tapered to reduce the side friction that develops as freezing occurs from the top downward (Berg et al. 1980b).

The base of each column is fitted with a porous stone and tubing leading from a source of water. These features and a Mariott tube allow us to control the position of the water table in the column. The soil column is placed inside a temperature-controlled jacket to minimize lateral heat losses and promote one-dimensional freezing or thawing.

The top of the column is attached to an air-activated piston, which applies the desired force (surcharge) to the soil surface through the surface heat-exchange plate. This plate is connected to a refrigerated bath via flexible tubing. The bath temperature is set manually to obtain the desired rate of freezing. A thermocouple is embedded in the surface heat-exchange plate. A linear-motion

potentiometer (LMP) is attached to the side of the soil column to monitor the amount of frost heave of the soil. Other instrumentation in the soil column includes thermocouples to monitor temperatures at selected positions and tensiometers to monitor pore-water pressures (moisture tension). The amount of water drawn into the soil is monitored manually once or twice per day, and the tensiometers, thermocouples and LMP are attached to a data collection system that records data hourly.

A dual gamma system was designed to be used with the soil column. It nondestructively monitors changes in density and moisture content with time during freezing and thawing of soils in the soil column. The system (Greatorex et al., in prep.) consists of two nuclear sources, an electronic detector to monitor gamma radiation from the sources, a tower to position the sources and detector vertically, and electronic equipment to control, monitor and record data from the system (Fig. 21).

### Test results

Several tests were run on soils from the Winchendon site and other soils, and the results were used as one source of data for validating and refining the frost-heave model, a mathematical model of coupled heat and moisture flow. During late 1984 and 1985, two special tests were conducted using the soil column and dual gamma system. Both special tests were designed to generate data to be used to validate and refine the recently developed thaw-settlement algorithm of the frost-heave model.

During previous tests using the soil column, frost heave was not substantial, even with highly frost-susceptible soil in the column. Therefore, for these two tests we froze 150–200 mm of soil in the multi-ring molds used in the laboratory frost-susceptibility test. Graves sand from the Winchendon test sections was used for the tests. The specimens were 150 mm in diameter by 150 mm high and were molded at a density of about  $1.52 \text{ gm/cm}^3$  for the tests. The soil specimens were frozen slowly from the top downward in a temperature-controlled cabinet; during freezing, about 20 mm of heave occurred.

The frozen soil specimens were machined to fit snugly inside the upper segment of the soil column, which was about 135 mm in diameter. The lower 900 mm of the soil column was filled with unfrozen Graves sand. Temperature sensors and tensiometers were installed at several locations in both the frozen and unfrozen portions of the soil column. An LMP was attached to the surface heat-exchange plate to monitor settlement as thawing progressed. A surcharge of about 7 kPa was applied at the surface using the air-actuated piston. The temperature in the jacket surrounding the soil column was maintained at about  $+0.5^\circ\text{C}$ . The water table was maintained at a depth of about 900 mm below the top of the sample throughout the tests.

After attaching a frozen soil segment to the rest of the soil column and installing the instrumentation, we circulated a mixture of ethylene glycol and water at  $-3^\circ\text{C}$  through the surface heat-exchange plate for several days. This caused the frost line to advance further and allowed temperatures and pore-water pressures in the soil to stabilize prior to the most important part of the test, whose objective was to monitor changes during thaw. For this purpose the temperature of the circulating fluid was gradually increased to about  $+2^\circ\text{C}$ . Thawing progressed slowly from the top downward during the tests, taking six days for

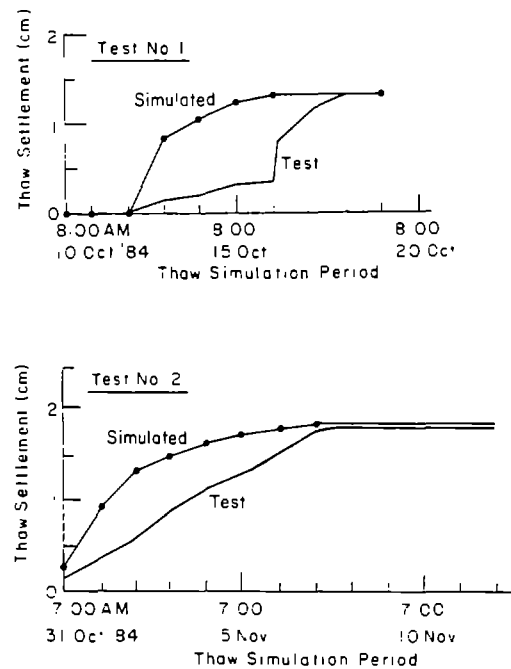


Figure 22. Thaw settlement in two soil-column tests on Graves sand.

complete thawing in Test 1 and about eight days in Test 2.

Figure 22 shows settlement during thawing in Tests 1 and 2, while Figure 23 shows the changes in temperature and moisture stress. Slight positive pressures were observed in both tests before the entire frozen layer was thawed. When thawing was complete, water drained downward into the underlying soil. The results from the tests were used as data sets for refining and validating the thaw-settlement portion of the frost-heave model. The simulated settlements, temperatures and moisture stresses obtained by use of the model agree very well with the observed values for Test 2. The simulation of Test 1 was not as accurate, mainly due to malfunctions of the laboratory surface-temperature controller and the data collection system. Because of these problems, reliable upper-boundary temperature data were unavailable for the simulation.

The dual gamma system was used periodically to monitor the moisture contents and density profiles in the soil column. Observations were closely spaced in the thawing portion of the column and 50 or 100 mm apart in the unfrozen portion.

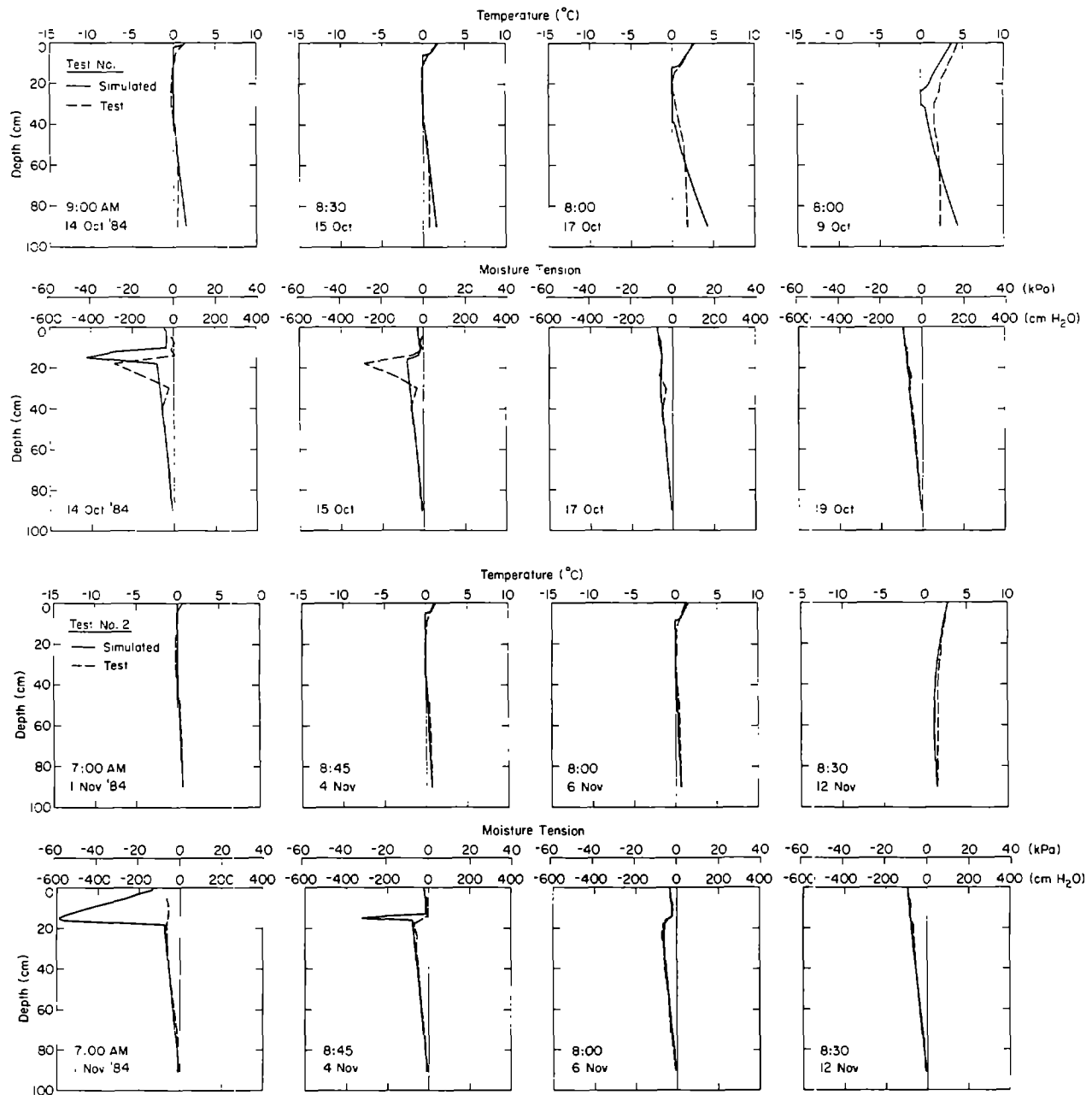


Figure 23. Temperatures and pore pressures in two soil-column tests on Graves sand. The solid lines are measurements; the dashed lines are simulations.

## MATHEMATICAL MODEL OF FROST HEAVE AND THAW SETTLEMENT

### Model development

We have reported the development of the model in Berg et al. (1980a, b), Guymon et al. (1980, 1981a, 1981b and in prep.) and Hromadka et al. (1981, 1982). The model assumes one-dimensional vertical heat and moisture flux. It is intended for use on problems of seasonal freezing and thawing of nonplastic soils beneath pavements in which

frost does not penetrate deeply into soils beneath the water table. Furthermore, it is intended for use where surcharge effects are not large (usually less than 60 kPa).

### Assumptions

The main assumptions of the model are:

- There are three distinct zones in a freezing soil: a frozen zone, a freezing zone and an unfrozen zone.
- Moisture transport in the unfrozen zone is

governed by the unsaturated flow equation based on Darcy's Law.

- Moisture flow is via liquid movement, and vapor flow is negligible.
- Moisture flow in the frozen zone is negligible, and there is no moisture loss or gain at the frozen soil surface.
- Soil deformations in the unfrozen zone are negligible.
- Soil pore-water pressures in the freezing zone are governed by an unfrozen-water-content factor.
- All processes are single valued; i.e., there is no hysteresis.
- Heat transport in the entire soil column is governed by the sensible-heat-transport equation including a convective term.
- The frozen zone is deformable for determining thermal parameters; i.e. the thermal conductivity is modified to compensate for the increased path length caused by frost heave.
- Salt exclusion processes are negligible; i.e., the unfrozen water content is constant with respect to temperature.
- Phase-change effects (freezing and thawing) and moisture effects can be modeled as decoupled processes.
- Freezing and thawing can be approximated as isothermal phase-change processes.
- All parameter and model uncertainty can be incorporated into a universal probability model applicable to a specific class of soils.
- Fluxes of heat and water are vertical, i.e. the model is one-dimensional and no lateral fluxes are considered.

#### Governing equations

The appropriate equation describing soil moisture flow consistent with the above assumptions is derived by substituting the extended Darcy moisture-flow law into the one-dimensional continuity equation for an incompressible fluid in porous media:

$$\frac{\partial}{\partial x} [K_H \partial h / \partial x] = \frac{\partial \theta_u}{\partial t} + \frac{\rho_i}{\rho_w} \frac{\partial \theta_i}{\partial t} \quad (1)$$

where the total hydraulic head  $h$  equals the sum of the pore pressure head ( $h_p = u / \rho_w$ , where  $u$  is the pore-water pressure and  $\rho_w$  is the density of water) and the elevation head ( $h_e = -x$ ). The coefficient of permeability  $K_H$  is a function of the pore pressure head in the unfrozen soil zone. In the right

side of the equation,  $\rho_i$  is the density of ice,  $\theta_i$  is the volumetric ice content, and  $\theta_u$  is the volumetric water content. The ice sink term,  $\rho_i \partial \theta_i / \rho_w \partial t$ , exists only for a freezing or thawing zone, and in these zones equation 1 is coupled to the heat-transport equation. The ice-sink term assumes that  $\theta_i$  is a continuous function of time.

It is computationally convenient to represent the soil-water characteristics as a known or assumed function relating pore-water pressure  $u$  and volumetric water content  $\theta_u$ . This is done by determining point values of  $\theta_u$  and  $u$  in the laboratory and by least-squares fitting of a function similar to that used by Gardner (1958) to the data:

$$\theta_u = \frac{n}{A_w |h_p|^\alpha + 1} \quad (2)$$

where  $n$  is the initial porosity and  $\alpha$  and  $A_w$  are best-fit parameters for each soil.

Similarly the coefficient-of-permeability function for an unsaturated soil is determined in the laboratory by determining point values of  $K_H$  and  $u$  for that soil and by least-squares fitting of Gardner's function to the data:

$$K_H = \frac{K_s}{A_k |h_p|^\beta + 1} \quad (3)$$

where  $K_s$  is the saturated permeability and  $A_k$  and  $\beta$  are the best-fit parameters.

A phenomenological relationship is assumed for adjusting the coefficient of permeability for unfrozen soils to represent conditions where ice is partially blocking soil pores (in the freezing zone). It is assumed that the coefficient of permeability in the freezing and frozen zones is

$$K_F = K_H(h_p) \cdot 10^{-E\theta_i} \text{ when } E\theta_i \geq 0 \quad (4)$$

where  $E$  is a parameter determined empirically. Taylor and Luthin (1978) and Jame (1978) used similar concepts to reduce the permeability in the freezing zone.

Frost heave is estimated from the total amount of ice segregation in the frozen zone by

$$\theta_s = \theta_i - (n - \theta_f) \quad (5)$$

where  $\theta_s$  = volumetric segregated ice content  
 $n$  = porosity  
 $\theta_f$  = residual unfrozen water content.

If  $\theta_s > 0$ , ice segregation has occurred and the

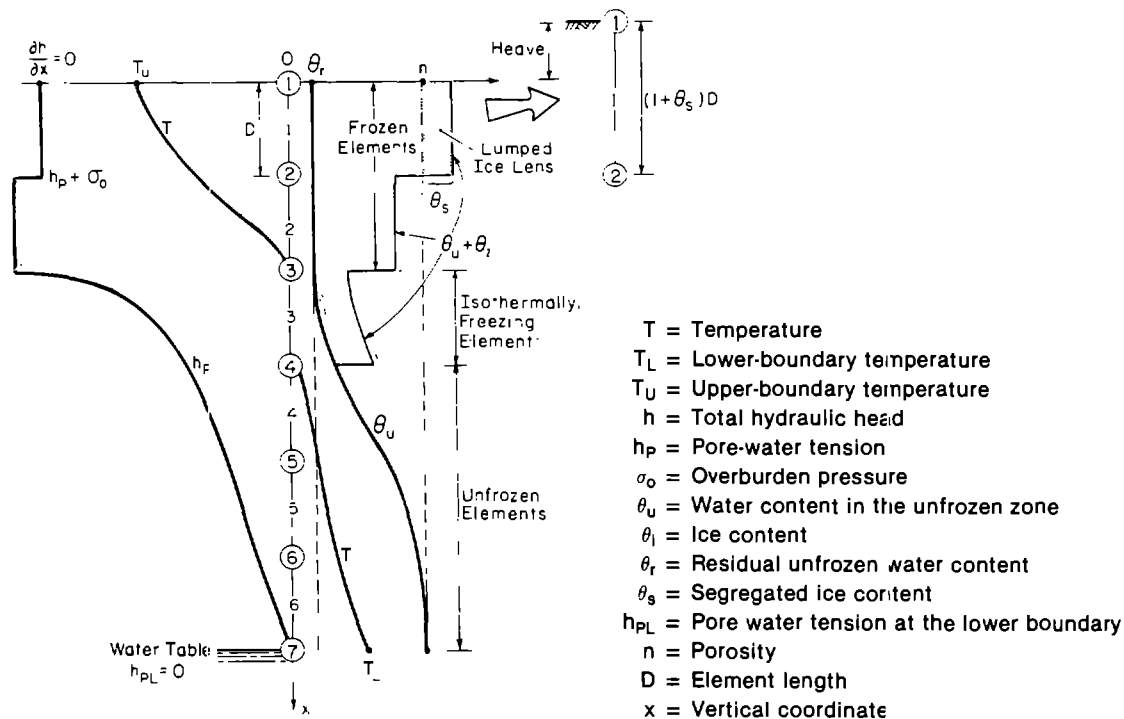


Figure 24. Typical model simulation result at a given time.

frost heave is computed by multiplying  $\theta_s$  by the zone thickness. Thaw consolidation from ice melting is the reverse process.

Figure 24 illustrates the solution of a freezing problem during a time step. The  $\theta_r$  parameter establishes the pore-water pressure at the freezing front for the solution of the moisture transport equation. The lower hydraulic boundary condition is usually the water table. Surcharge and overburden effects  $\sigma_o$ , which tend to restrain frost heave, are modeled by reducing the pore-water tension at the ice-segregation front by the pressure of the overlying material and surcharge.

#### Conceptual basis for thaw-settlement algorithm

The thaw-settlement portion of the model is discussed separately because of the importance of this submodel for the evaluation of thaw weakening of soils beneath pavements, a major objective of this project. The concepts advanced by Morgenstern and Nixon (1971) provide the framework for the thaw-settlement and pore-water-pressure algorithm presented here. In the past the limited availability and poor quality of laboratory data inhibited the development of accurate and tested thaw-settlement models. Additional data were collected during this study using the CRREL soil col-

umn to test the adopted thaw-settlement algorithm.

The Morgenstern and Nixon model is based on well-known theories of heat conduction and linear consolidation of compressible soils. Terzaghi's one-dimensional consolidation theory was applied to develop a moving-boundary solution applicable to permafrost soils that thaw and consolidate under the application of load. A closed-form solution was obtained.

Our application of the model is directed to layered systems of well-compacted soils. Consequently the application is restricted to winter heaving of subgrade soils and spring thaw settlement originating in those same soils with no net consolidation or change in pavement elevation occurring over a sequence of several years of freeze-thaw action.

A departure from the Morgenstern and Nixon model is the solution of the linear governing equation of excess pore-water pressure (Terzaghi's equation) numerically rather than exactly. The numerical code for this solution already exists in the frost-heave model. This method allows more flexibility in handling the upper-surface pore-water-pressure boundary condition. A second departure from the Morgenstern and Nixon method is the use of a more general heat transport equation.

To determine the thaw settlement, equation 1,

which governs the moisture flow during frost heave, was modified to include a temporal void-ratio term (Lambe and Whitman 1979):

$$K_H \frac{\partial^2 h}{\partial x^2} = \frac{\partial \theta_u}{\partial t} + S m_v \gamma_w \frac{\partial h}{\partial t} + \frac{e_i}{e_w} \frac{\partial \theta_i}{\partial t} \quad (6)$$

where  $S$  is the degree of saturation and  $m_v$  is the coefficient of volume compressibility.

Equation 6 is the basis of the algorithm for estimating thaw settlement and pore-water pressure during and after thawing. When soil-surface temperatures are above freezing and the upper element is fully saturated, soil-surface pore-water pressures are set to a specified pressure, which is usually atmospheric plus the excess pressure from overburden effects. However, the model does have the ability to apply a specified lesser positive pressure representing drainage upward through a slowly leaking pavement overlying the base course material. When the upper soil element becomes partly drained ( $S < 100\%$ ) or when the surface element refreezes, the soil-surface boundary condition for the moisture equation is reset to a no-flux boundary condition.

As thawing progresses downward, each discrete soil element is checked to determine the degree of saturation. If excess pore-water pressure exists, water in excess of the initial porosity is treated as a source, forcing an upward drainage of water. The hydraulic conductivities of underlying frozen zones are determined by equation 3, with the parameters  $A_k$  and  $\beta$  evaluated by laboratory tests and the pore-water pressure determined by means of equation 2 with  $\theta_u$  set equal to  $\theta_r$ .

When the soil column is completely thawed and reconsolidated, free downward drainage occurs in accordance with equation 1, and the no-flux surface boundary condition is assumed to persist.

#### Boundary and initial conditions

The model requires auxiliary conditions as follows:

- Initial conditions for pore pressure, ice content and temperature.
- Soil-surface boundary conditions for pore pressure and temperatures (which may vary with time).
- Lower boundary conditions for pressure and temperature (which may vary with time).

While there are many possibilities for incorporating boundary conditions in the model to suit specific applications, the CRREL version of the model has the features discussed below.

The upper-boundary pore-water pressure is fixed at a specific value with respect to time during freezing. Prior to freezing it varies according to equation 1, while after thawing it varies according to equation 6.

The lower pore-pressure boundary condition is usually a set of discrete pore-water pressures (tensions) at specific times that are related to the water table elevation. Intermediate times and pore-water pressures are linearly interpolated.

The upper temperature boundary condition consists of a set of specified step functions such as mean daily air temperatures. These values are multiplied by a factor to represent soil-surface temperatures, in a manner similar to the Corps of Engineers  $n$ -factor approach for seasonal freezing indexes.

Bottom temperature boundary conditions consist of a set of times and temperatures. Temperatures are linearly interpolated at intermediate times.

#### Numerical approach

Numerical solution of the governing equations, subject to their respective boundary and initial conditions, is by the nodal domain integration method (Hromadka et al. 1982). The one-dimensional solution domain is divided into a number of variable-length finite elements where parameters are assumed to be temporarily constant but may vary from element to element and from time to time. Figure 25 illustrates the division of a vertical column into elements and nodes. The state varia-

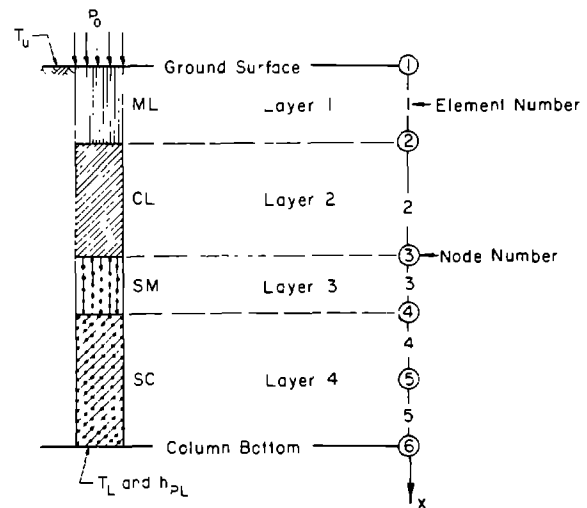


Figure 25. Nonuniform soil profile divided into elements and nodes and showing boundary conditions.

ble in each element is assumed to be described by a linear basis function such that the state variable is continuous throughout the solution domain. The time-domain solution is by either the Crank-Nicolson approach or the fully implicit method.

Computation is initiated by giving the initial conditions, and the solution is advanced in time. At specified times nonlinear parameters are updated.

### Probabilistic concepts

If this one-dimensional model were perfect, it would predict exactly the amount of frost heave and frost penetration at a point with time. However, it would not account for spatial variations in the amounts of frost heave and the degree of thaw weakening caused by differences in the thermal and hydraulic properties, in turn caused by differences in density, moisture content and soil-particle size and arrangement. We assume that the model is not perfect and combine uncertainties in the model with variations in the soil via probabilistic methods. The uncertainty is arbitrarily grouped into four general areas:

- Errors due to the choice of the model, including the choice of a numerical analog.
- Errors due to spatial and temporal variations in the soil properties.
- Errors due to inadequate boundary conditions and to the choice of initial conditions.
- Errors due to the selection of parameter values.

Errors due to the choice of a model are probably indeterminate by strictly analytical methods. Choosing a model is probably best left to experience with application of the model for a number of known laboratory and field conditions. Errors associated with the choice of a numerical analog were readily examined, as were errors associated with spatial and temporal variations in the soil properties (Guymon et al. 1981b and in prep., Hromadka et al. 1982). We concluded that one numerical technique had little advantage over others and the model is relatively insensitive to spatial discretization. The model is very sensitive to temporal changes, and we found that for most solutions a time step of 0.2 hr and a parameter update frequency of 1 hr are satisfactory.

Errors associated with inadequate boundary and initial conditions, and particularly with parameter values, require special attention due to the probabilistic nature of their variations. For this reason, probabilistic theory is applied to consider the uncertainties and variations.

Most investigations of this nature use hundreds or even thousands of computer simulations. This type of stochastic analysis can be very expensive, particularly if variations are significantly different for different soil types or boundary or initial conditions. The probabilistic method used in the model, discussed in detail in Guymon et al. (1981b and in prep.), eliminates the need for such large numbers of computer simulations.

### Model verification

Model verification has been a continuing process since completion of early work on formulating the model reported by Berg et al. (1980a). This report contained early verification of decoupled components of the model (e.g. sensible heat transport) against analytical solutions using linearized computer simulations (Fig. 26). As verification work progressed, it was found necessary to refine the computer code to more accurately simulate pore pressures, temperatures and frost heave. Guymon et al. (1980) further reported on verification efforts using Fairbanks silt as a test case. Subsequently Guymon et al. (1981a, 1981b and in

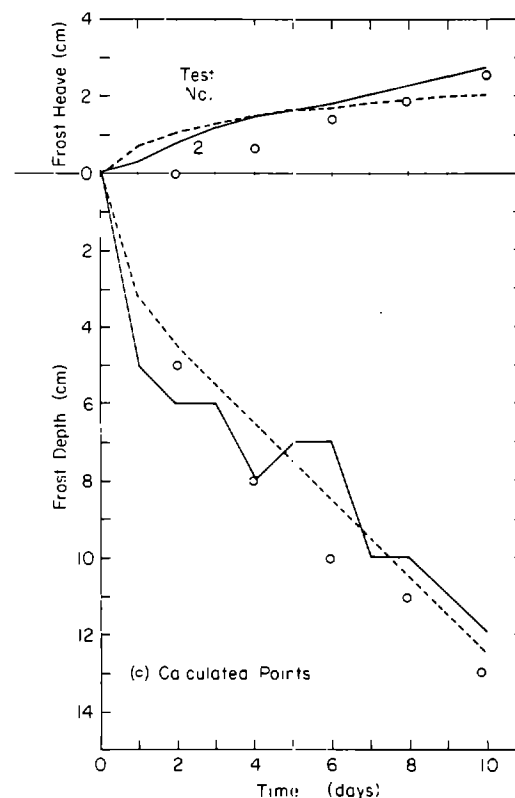


Figure 26. Measured and simulated frost depth and frost heave, laboratory soil-column test on Fairbanks silt.

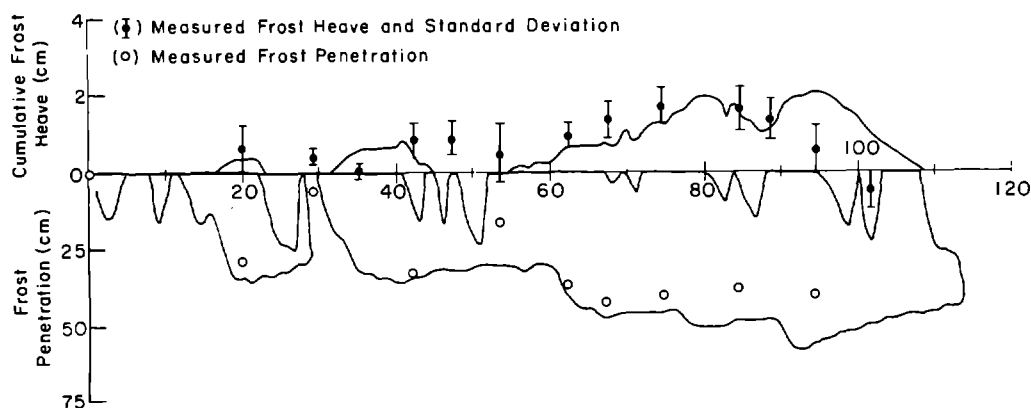


Figure 27. Measured and simulated frost depth and frost heave, Taxiway B, Albany County Airport, 1979-80.

prep.) presented much greater detail in verifying the model against laboratory and field data. Figure 27 illustrates calculated and measured values of frost heave and frost penetration with time from one of the test sections at the Albany County Airport. Additional verification results are presented below.

#### Discussion

The model produced good results for soils ranging from silts to relatively coarse-grained and marginally frost-susceptible soils. Moreover, these results have been compared with carefully controlled laboratory data as well as less-precise field data for three locations.

To achieve such results, however, good estimates of hydraulic parameters are required. Judgment is required in assigning appropriate values, as there may be considerable variations in even the most carefully measured soil parameters, particularly unsaturated hydraulic conductivity.

The modeling exercise also requires calibration of the hydraulic-conductivity correction factor  $E$ , a phenomenological correction factor for soil in the freezing zone. This factor is used as the primary calibration parameter to achieve the results presented here. If measurements of hydraulic conductivity for partly frozen soil were available or could be easily obtained, it is likely that those data could be used instead of the phenomenological relationship now incorporated in the model.

The model also requires an estimate of the moisture tension in the freezing zone. This is done indirectly by selecting a residual (unfrozen) water content for the frozen zone and by calculating the corresponding pore-water tension by the Gardner equation. Generally values of residual water con-

tent are selected so that the moisture tension is 75-100 kPa. The actual values may be soil specific and much greater or lower than this range.

Even if more-precise scientific knowledge were available for this function, calibration might still be required. There is no model in existence for porous-media flow processes that does not require calibration to improve the confidence limits so that the deterministic solution becomes relatively precise. Hypothetical solutions of such problems using assumed parameters have a considerable error, which for some porous-media problems may be tolerable in the engineering analysis process. Usually engineering judgment and experience are exercised to infer the level of certainty of such computations. This need is evident in the problem considered here.

We believe that the model simulates phenomena in the freezing zone adequately for our present engineering purposes and that it will meet the need of practicing pavement engineers for predicting frost heave and some of the parameters influencing thaw weakening of pavement systems. The development of a model more closely linked to accepted concepts of soil physics awaits a more complete understanding and formulation of processes in the freezing zone. It would also require additional computer time and expense to solve a more complex formulation of the processes, and additional time, equipment and expense for conducting laboratory tests to define additional soil parameters.

The output from the model includes cumulative frost heave with time at the surface, subsurface temperatures and pore-water pressures. The predicted frost heave can be used directly to aid in selecting an appropriate pavement design by relating



it to pavement roughness criteria. Temperatures are used to determine the positions of the freezing and thawing zones, and temperatures and pore-water pressures are used in empirical equations developed from laboratory tests to estimate resilient-modulus values for layers within the pavement system at various times of the year. The resilient-modulus data are then used in a pavement structural response model, where output can be related to pavement performance criteria. Examples of this application are presented later in this report.

### **SEASONAL VARIATION IN THE RESILIENT MODULUS OF GRANULAR SOILS**

In areas of seasonal frost the supporting capacity of subgrade soils and unbound base and sub-base materials for roads and airfields can vary widely during freeze-thaw cycling and the subsequent spring and summer recovery period. In this phase of the research we sought to evaluate the seasonal fluctuations in material properties for six soils from the Winchendon test site and five soils from pavements at the Albany County Airport test site. The investigations focused on the underlying cause of premature distress in pavement systems that are susceptible to frost—the reduction of the resilient modulus of subgrade soils and unbound base courses during and following spring thaws. In this context the resilient modulus is conventionally defined as the deviator stress divided by the resilient strain (i.e. the recoverable strain). The research was concerned with frost-susceptible granular soils exhibiting little or no cohesion and a high degree of nonlinear (i.e. stress-dependent) mechanical behavior. The research objective was to develop laboratory methods for characterizing the seasonal changes in the resilient modulus of such materials throughout a complete annual cycle. Field tests were conducted to validate the laboratory methods.

Repeated-load triaxial tests were performed to determine the resilient characteristics of the materials under conditions simulating those during the field tests. The laboratory triaxial tests were performed on soils in the frozen, thawed, recovering and recovered conditions. Empirical relationships were then generated by standard statistical techniques to express the resilient modulus  $M_r$  as a function of the density, the soil-moisture tension and the stresses imposed in the triaxial tests. For frozen soil and asphalt concrete, temperature is also a key parameter.

For validation purposes, field tests were used to determine the surface deflection response of paved soil test sections under plate loads. Surface deflection basins were measured under loads imposed by a repeated-load plate-bearing (RPB) apparatus and a falling-weight deflectometer (FWD). The tests were performed at critical times between late fall and late spring to characterize the variation in load response throughout the freeze-thaw-recovery cycle.

The validity of the laboratory results was then examined by comparing the measured deflection basins with deflection basins calculated for the test section using the expressions for resilient modulus developed from the laboratory tests. In using these expressions, temperatures and moisture tensions measured at the time of each field loading test were applied to evaluate the resilient modulus. Layered elastic analyses of the test sections under the conditions prevailing during each field loading test yielded stresses, strains and resilient vertical displacements throughout the system; calculated surface deflection basins were thus generated and compared to the deflection basins actually measured in the field.

Interim results were given by Cole et al. (1981) and Johnson et al. (1982). Detailed procedures, results and analyses of repeated-load triaxial tests, and of field in-situ plate-loading tests and the corresponding deflection basin analyses, are given in a four-part report series by Cole et al. (1986 and in prep.) and Johnson et al. (1986a, b).

#### **Characterization by laboratory testing**

The objective of this phase of the work was to develop procedures for obtaining realistic expressions for the resilient modulus of granular soils in the frozen, thawed and recovered states in terms of the significant variables. The testing and analytical techniques we have developed allow us to simulate in the laboratory the gradual recovery of stiffness experienced in the field as a frost-susceptible soil drains, consolidates and desaturates after thawing.

#### *Experimental approach*

The experimental approach called for repeated-load triaxial tests on all the asphalt concrete and test soils from both test sites. We obtained field cores of the asphalt concrete and of the finer-grained soils in the frozen state. We also sampled several test sections at the Winchendon site before the subsoils froze, to characterize the material after it had fully recovered from the previous winter's freezing cycle. In the case of glacial till or

gravel, where core samples could not be obtained, we reconstituted specimens in the laboratory and subjected them to open-system freezing at a rate of 25 mm/day to produce the appropriate conditions for testing.

Load cycles on the soils were applied using two waveforms to simulate the loading pulses associated with our two field-testing devices: the falling-weight deflectometer (FWD) and the repeated-load plate-bearing (RPB) apparatus. Two hundred load cycles were applied at each level of confining and deviator stress used in the laboratory tests, and the resilient modulus and resilient Poisson's ratio were calculated when a nominally steady-state response was achieved.

By performing these tests under a variety of temperature and moisture conditions comparable to those observed in the field, we were able to characterize the resilient properties and generate analytical expressions in terms of the significant variables.

The terminology used to describe the state of the soils is as follows. "Frozen" refers to material with at least some pore ice present, and "thawed" refers to material having only liquid pore water but that is still suffering from the effects of a freezing cycle (i.e. it has not drained or consolidated to its prefreezing state and is consequently still in a weakened condition). The term "recovered" refers to material that by means of drainage, consolidation and desaturation has been restored to the moisture and density conditions (and hence stiffness) prevailing before the start of a freezing cycle. Details of the experimental procedures are given in Cole et al. (1986).

#### Advancements

A number of significant advancements in triaxial testing equipment and procedures have allowed us to simulate the thaw and recovery process in the laboratory. The key variable in the recovery process is soil-moisture tension. As a soil drains after thawing, it first reconsolidates to a condition of zero pore-water pressure. Following this phase, gradual desaturation occurs, the moisture tension rises, and the resilient modulus increases. We developed a system, using removable triaxial-cell bases equipped with tensiometers, that allowed us to retest a given specimen several times at increasing levels of moisture tension, thus simulating the changes observed in the field. Each specimen remained mounted on its base throughout the testing sequence, and excessive handling was thus avoided.

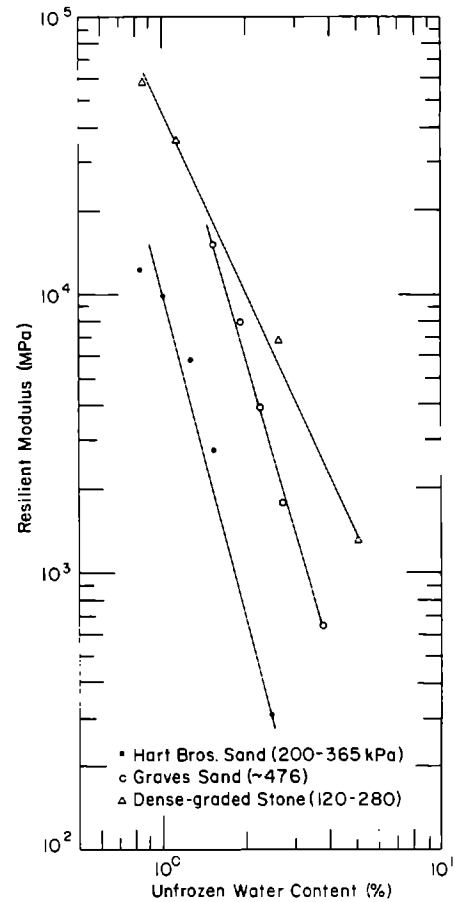


Figure 28. Resilient modulus vs unfrozen water content for three frozen Winchendon soils tested at 69 kPa confining stress and the indicated ranges of deviator stresses.

The ability to perform sequential tests allowed us to simulate the stiffness recovery in the laboratory with a relatively small number of specimens. We generally tested specimens four times, which allowed us to cover the full range of field conditions with each specimen. The use of moisture tension as the primary means of describing the soil state has proven to be effective since it strongly influences the resilient modulus and is relatively easily monitored in both the field and the laboratory.

Other developments at CRREL in the use of the pulsed nuclear magnetic resonance technique on frozen soils\* provided us with information on the unfrozen water content of the frozen soils tested in this program. The unfrozen water content (Fig. 28) was found to have a profound influence on the

\* Personal communication with A. Tice, 1983.

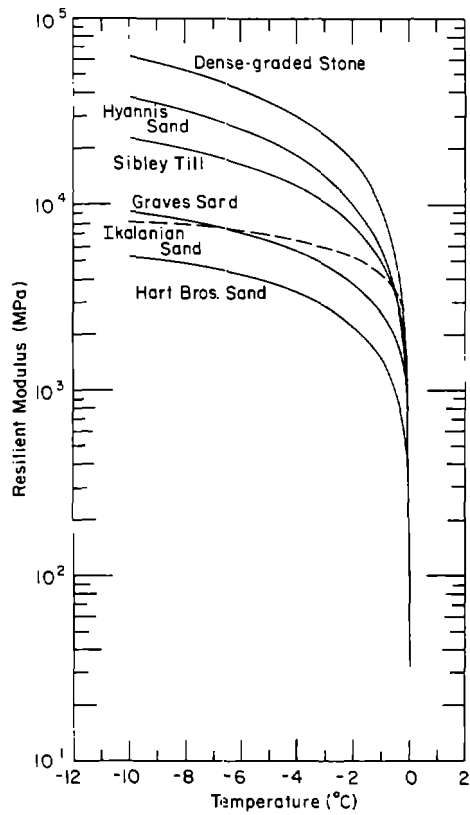


Figure 29. Resilient modulus vs temperature for the six Winchendon test soils in the frozen state. Curves are generated by regression equations based on unfrozen-water-content expressions.

resilient modulus of material in the frozen state and was consequently used as the key variable in the empirical modeling effort. The equations are of the form

$$M_r = C_1(w_u/w_t)^{C_2} \quad (7)$$

where  $M_r$  = resilient modulus  
 $C_1, C_2$  = constants  
 $w_u$  = unfrozen water content, expressed as a function of temperature  
 $w_t$  = total gravimetric water content.

The unfrozen water content is expressed (Cole 1984) by an equation of the form

$$w_u = \alpha(-T)^\beta \quad (8)$$

where  $\alpha$  and  $\beta$  are regression constants and  $T$  is temperature. This constitutes the first use of an unfrozen-water-content term in a resilient-modulus expression, and the results have been very

satisfactory. The expressions are relatively simple and mathematically well behaved, and they can be extrapolated to lower temperatures with reasonable confidence. This analytical approach requires fewer laboratory tests to obtain a useful expression. Figure 29 shows a plot of modulus vs temperature for the six Winchendon soils.

Standard statistical techniques have been used in this work to generate empirical expressions for the resilient modulus in terms of the unfrozen water content for the frozen case and in terms of the moisture tension, the applied stress and in some cases the dry density for the thawed cases.

In some cases we have applied the commonly used bulk-stress model for the stress dependency of a nonlinear material, which is of the form

$$M_r = K_1 J_1^{K_2} \quad (9)$$

where  $K_1$  and  $K_2$  are constants and  $J_1$  is the first stress invariant (sum of the principal stresses, equal to the bulk stress  $\ell$ ). We have also employed a somewhat more complex stress function involving the second stress invariant and the octahedral shear stress, of the form

$$M_r = K_1(J_2/\tau_{oct})^{K_2} \quad (10)$$

where  $J_2$  = second stress invariant  
 $= \sigma_1\sigma_2 + \sigma_2\sigma_3 + \sigma_1\sigma_3$   
 $\tau_{oct}$  = octahedral shear stress  
 $= \frac{1}{3}[(\sigma_1 - \sigma_2)^2 + (\sigma_2 - \sigma_3)^2 + (\sigma_1 - \sigma_3)^2]^{1/2}$   
 $\sigma_1, \sigma_2, \sigma_3$  = principal stresses.

The stress function of equation 10 is unique in that it accounts for the effects of both confining pressure and the principal stress ratio on the modulus in a manner appropriate for many granular materials.

Figure 30 shows a plot of modulus vs bulk stress for a thawed Winchendon test soil (Hyannis sand). The bulk-stress model does not account for the fact that, for certain types of soil, the modulus decreases with increasing principal stress ratio. The stress function given in equation 10, however, accounts for the influence of the stress ratio and thus gives a more efficient linear representation of the data (Fig. 31).

### Results

Analysis of the laboratory test data for each soil yielded equations applicable to the frozen state and the thawed state. The frozen-state equation is in fact valid up to and including the point of com-

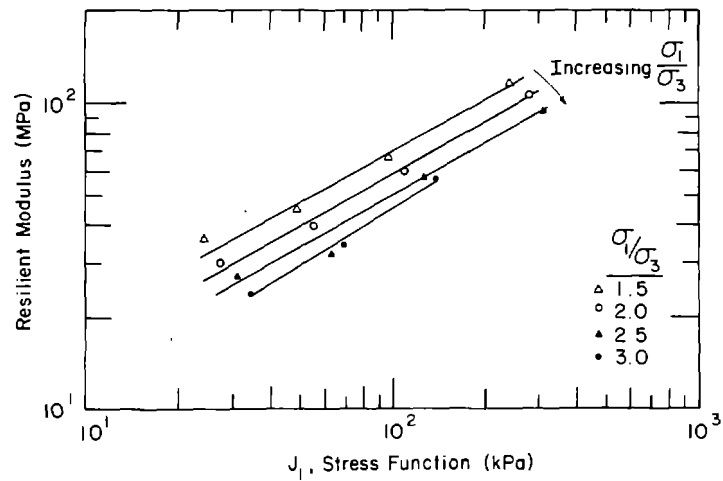


Figure 30. Resilient modulus of thawed Hyannis sand vs  $J_1$  (first stress invariant, equal to bulk stress  $\theta$ ) for several values of principal stress ratio, demonstrating the tendency for the modulus to decrease with increasing stress ratio when the confining stress  $\sigma_3$  remains fixed.

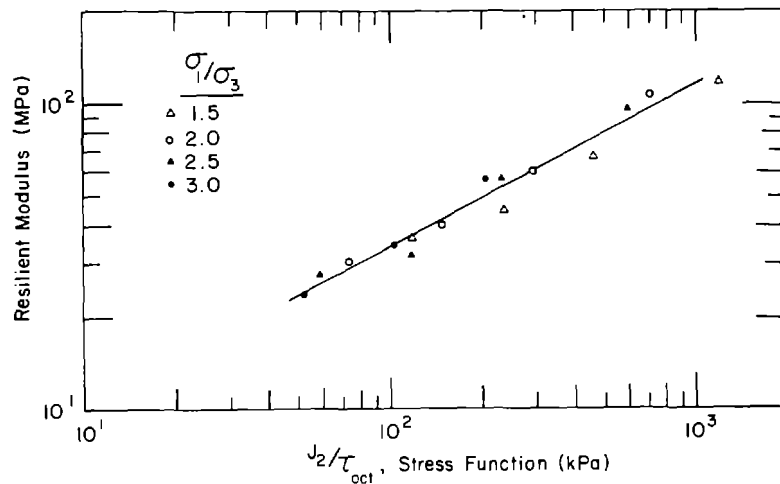


Figure 31. Resilient modulus vs  $J_2/\tau_{oct}$  for the test data given in Figure 30.

plete thaw, at which point the expressions yield the average modulus value observed in the “as thawed” condition (i.e. prior to any drainage). A significant feature of this approach is that it yields a continuous function up to the point of thawing, because we included appropriate data points from the thawed state in the analysis.

The laboratory testing sequence mentioned above generated data that allowed us to model the post-thaw recovery process with a single equation employing terms for stress, soil-moisture tension and dry density. The increasing stiffness associated with the recovery phase is predicted through

the moisture-tension term, which is incorporated in the coefficient  $K_1$ . Figure 32 shows how moisture tension affects the term  $K_1$ , and thus the moduli, in equations 9 and 10 as evaluated by means of regression analyses (Tables 4 and 5) for several Albany Airport test soils. Earlier work (Cole et al. 1981) demonstrated that  $K_2$  is statistically independent of the moisture tension.

Tables 4 and 5 show the results of the regression analyses on the asphalt concrete and all test soils for both the frozen and thawed conditions. In general, the stress function  $J_2/\tau_{oct}$  produced a higher coefficient of determination ( $R^2$ ) than the  $J_1$  (bulk stress) model.

**Table 4. Results of regression analyses, asphalt concrete and test soils from Winchendon.**

Material	Load pulse	Regression equation	n	R <sup>2</sup>	Std. error	Eq. no.
<b>Asphalt concrete</b>						
	RPB	$M_r(\text{MPa}) = \exp[9.204 - 5.552 \times 10^{-3}T - 9.744 \times 10^{-4}T^2]$	85	0.97	0.287	1
	Haversine	$M_r(\text{MPa}) = \exp[9.183 - 7.47 \times 10^{-2}T] f^{0.1777}$	158	0.81	0.469	2
	FWD	$M_r(\text{MPa}) = \exp[9.429 - 7.47 \times 10^{-2}T]$	—	—	—	3
<b>Natural subgrade</b>						
	RPB and FWD	$M_r(\text{MPa}) = 8.829 f_i(\sigma)^{0.708}$	65	0.67	0.235	4
	RPB and FWD	$M_r(\text{MPa}) = 20.74 f_z(\sigma)^{0.352}$	65	0.76	0.201	5
<b>Graves sand</b>						
Frozen	RPB	$M_r(\text{MPa}) = \exp(9.677 - 1.0314T - 0.0708T^2)(\tau_{\text{ocf}}/\sigma_o)^{-0.682}$	56	0.88	0.332	7
	RPB	$M_r(\text{MPa}) = 39.1(w_u/w_t)^{-1.79}$	95	0.91	0.502	8
	FWD	$M_r(\text{MPa}) = 32.14(w_u/w_t)^{-1.96}$	73	0.95	0.446	9
Thawed	RPB	$M_r(\text{MPa}) = 2.139 \times 10^6 f(\psi)^{-2.7925} f_i(\sigma)^{0.462}$	186	0.76	0.209	10
	FWD	$M_r(\text{MPa}) = 9.27 \times 10^5 f(\psi)^{-2.60} f_i(\sigma)^{0.477}$	222	0.71	0.224	11
	RPB	$M_r(\text{MPa}) = 6.68 \times 10^4 f(\psi)^{-2.2948} f_z(\sigma)^{0.414}$	186	0.89	0.144	12
Recovered	FWD	$M_r(\text{MPa}) = 1.47 \times 10^6 f(\psi)^{-2.75} f_z(\sigma)^{0.413}$	222	0.86	0.157	13
	RPB	$M_r(\text{MPa}) = 6.89 f_i(\sigma)^{0.418}$	36	0.76	0.247	14
	RPB	$M_r(\text{MPa}) = 4.80 f_z(\sigma)^{0.4046}$	36	0.87	0.185	15
<b>Ikalanian sand</b>						
Frozen	RPB	$M_r(\text{GPa}) = \exp[13.74 - (0.820)T - (0.0538)T^2 - (0.8378)w + (0.04416)w^2](\tau_{\text{ocf}}/\sigma_o)^{-0.382}$	62	0.90	0.308	16
	RPB	$M_r(\text{MPa}) = 86.4(w_u/w_t)^{-1.32}$	87	0.92	0.749	17
Thawed	RPB	$M_r(\text{MPa}) = 8.129 \times 10^4 f(\psi)^{-3.324} f(\gamma_d)^{11.578} f_i(\sigma)^{0.490}$	119	0.84	0.323	18
	RPB	$M_r(\text{MPa}) = 3.021 \times 10^4 f(\psi)^{-3.266} f(\gamma_d)^{11.634} f_z(\sigma)^{0.442}$	119	0.89	0.276	19
Recovered	RPB	$M_r(\text{MPa}) = 5.69 \times 10^6 f(\psi)^{-3.118} f_i(\sigma)^{0.537}$	38	0.88	0.205	20
	RPB	$M_r(\text{MPa}) = 2.405 \times 10^6 f(\psi)^{-2.918} f_z(\sigma)^{0.442}$	38	0.84	0.238	21
<b>Hart Brothers sand</b>						
Frozen	FWD	$M_r(\text{MPa}) = 38.28(w_u/w_t)^{-1.752}$	88	0.95	0.53	22
	RPB	$M_r(\text{MPa}) = 4.085 \times 10^1 (w_u/w_t)^{-1.59}$	99	0.92	0.623	22
	FWD	$M_r(\text{MPa}) = 8.05 \times 10^{-2} f(\gamma_d)^{7.64} f_z(\sigma)^{0.365} (w_u/w_t)^{-1.97}$	88	0.97	0.445	23
Thawed	FWD	$M_r(\text{MPa}) = 4.689 \times 10^{-1} f_i(\sigma)^{0.484} (w_u/w_t)^{-1.38}$	88	0.96	0.464	25
	RPB	$M_r(\text{MPa}) = 2.97 \times 10^3 f(\psi)^{-3.063} f(\gamma_d)^{5.986} f_z(\sigma)^{0.453}$	174	0.71	0.280	26
	RPB	$M_r(\text{MPa}) = 1.269 \times 10^5 f(\psi)^{-3.089} f(\gamma_d)^{7.023} f_z(\sigma)^{0.453}$	174	0.87	0.185	27
	FWD	$M_r(\text{MPa}) = 3.93 \times 10^4 f(\psi)^{-2.67} f(\gamma_d)^{6.18} f_i(\sigma)^{0.457}$	164	0.67	0.292	28
	FWD	$M_r(\text{MPa}) = 3.81 \times 10^4 f(\psi)^{-2.817} f(\gamma_d)^{7.43} f_z(\sigma)^{0.375}$	164	0.67	0.292	29
<b>Hyannis sand</b>						
Frozen	RPB	$M_r(\text{MPa}) = 0.68 f(\gamma_d)^{11.0} (w_u/w_t)^{-2.12}$	69	0.96	0.536	30
	RPB	$M_r(\text{MPa}) = 33.45(w_u/w_t)^{-2.03}$	69	0.95	0.617	31
Thawed	FWD	$M_r(\text{MPa}) = 7.147 \times 10^4 f(\psi)^{-1.782} f_z(\sigma)^{0.264}$	128	0.71	0.129	32
	FWD	$M_r(\text{MPa}) = 3.57 \times 10^7 f(\psi)^{-3.276} f_z(\sigma)^{0.3628}$	61	0.74	0.194	33
<b>Dense-graded stone</b>						
Frozen	RPB	$M_r(\text{MPa}) = 82.27(w_u/w_t)^{-2.03}$	32	0.97	0.413	34
Thawed	RPB	$M_r(\text{MPa}) = 1.56 \times 10^5 f(\psi)^{-1.76} f_z(\sigma)^{0.136}$	64	0.65	0.202	35
	RPB	$M_r(\text{MPa}) = 7.17 \times 10^4 f(\psi)^{-1.589} f_z(\sigma)^{0.1725}$	64	0.65	0.203	36
<b>Sibley till</b>						
Frozen	RPB	$M_r(\text{MPa}) = 1.01 \times 10^2 (w_u/w_t)^{-3.446}$	108	0.87	0.71	37
Thawed	RPB	$M_r(\text{MPa}) = 7.47 \times 10^6 f(\psi)^{2.829} f_z(\sigma)^{0.192}$	118	0.63	0.283	38
	RPB	$M_r(\text{MPa}) = 1.29 \times 10^7 f(\psi)^{-2.84}$	118	0.54	0.313	39

**NOTES:**

RPB = repeated-load plate-bearing apparatus waveform

FWD = falling-weight deflectometer waveform

n = number of points

R<sup>2</sup> = coefficient of determination

M<sub>r</sub> = resilient modulus

f = load wave frequency

f<sub>i</sub>(σ) = (J<sub>i</sub>/σ<sub>o</sub>)

σ = stress (kPa)

f<sub>z</sub>(σ) = [(J<sub>z</sub>/τ<sub>ocf</sub>)/σ<sub>o</sub>]

σ<sub>o</sub> = 1 kPa

w<sub>u</sub> = unfrozen water content

w<sub>t</sub> = total water content

T = θ/θ<sub>o</sub>

θ = temperature (°C)

θ<sub>o</sub> = 1 °C

f(ψ) = [(101.38 - ψ)/ψ<sub>o</sub>]

γ = moisture tension (kPa)

ω<sub>o</sub> = 1 kPa

γ<sub>d</sub> = dry unit weight (Mg/m<sup>3</sup>)

f(γ) = γ/γ<sub>o</sub>

γ<sub>o</sub> = 1 Mg/m<sup>3</sup>

**Table 5. Results of regression analyses, asphalt concrete and test soils from Albany Airport.**

Material	Load pulse	Regression equation	n	R <sup>2</sup>	Std. error	Eq. no.
<b>Taxiway A</b>						
Asphalt/concrete	FWD	$\dagger M_r(\text{MPa}) = 1.84 \times 10^4 \exp[-3.80 \times 10^{-2} T - 9.14 \times 10^{-4} T^2]$	88	0.97	0.19	1
	RPB	$M_r(\text{MPa}) = 1.01 \times 10^4 \exp[-6.50 \times 10^{-2} T - 6.50 \times 10^{-4} T^2]$	93	0.98	0.24	2
	Haversine	$M_r(\text{MPa}) = 1.09 \times 10^4 \exp[-4.75 \times 10^{-2} T - 7.81 \times 10^{-4} T^2] / \text{Hz}^{0.20}$	280	0.97	0.22	3
Thawed base	FWD/RPB	$\dagger M_r(\text{MPa}) = 1.10 \times 10^4 [f(\psi)]^{-2.40} f_i(\sigma)^{0.30}$	222	0.82	0.16	4
		$M_r(\text{MPa}) = 4.44 \times 10^4 [f(\psi)]^{-2.20} f_i(\sigma)^{0.37}$	222	0.82	0.16	5
		$M_r(\text{MPa}) = 3.68 \times 10^4 [f(\psi)]^{-2.15} f_i(\sigma)^{0.30} f(\gamma_d)^{3.44}$	222	0.84	0.16	6
		$M_r(\text{MPa}) = 2.56 \times 10^4 [f(\psi)]^{-1.99} f_i(\sigma)^{0.37} f(\gamma_d)^{2.90}$	222	0.82	0.16	7
Frozen base		$\dagger M_r(\text{MPa}) = 1.89 \times 10^4 (w_u/w_t)^{-4.82}, w_u = 3 \times 10^{-2}(-T)^{-0.25}, w_t = 0.075$	78	0.78	0.66	8
Thawed subbase	FWD/RPB	$\dagger M_r(\text{MPa}) = 2.07 \times 10^4 [f(\psi)]^{-3.05} f_i(\sigma)^{0.29}$	149	0.80	0.20	9
		$M_r(\text{MPa}) = 4.35 \times 10^4 [f(\psi)]^{-2.72} f_i(\sigma)^{0.37}$	149	0.80	0.20	10
		$M_r(\text{MPa}) = 1.39 \times 10^{10} [f(\psi)]^{-3.38} f_i(\sigma)^{0.29} f(\gamma_d)^{-7.00}$	149	0.82	0.20	11
		$M_r(\text{MPa}) = 8.00 \times 10^4 [f(\psi)]^{-2.99} f_i(\sigma)^{0.37} f(\gamma_d)^{-5.55}$	149	0.82	0.19	12
Frozen subbase		$\dagger M_r(\text{MPa}) = 8.18 \times 10^4 (w_u/w_t)^{-4.02}, w_u = 3 \times 10^{-2}(-T)^{-0.25}, w_t = 0.055$	53	0.70	0.84	13
Non-frozen subgrade	FWD/RPB	$\dagger M_r(\text{MPa}) = 1.34 \times 10^4 [f(\psi)]^{-1.50} f_i(\sigma)^{0.33}$	262	0.80	0.80	14
		$M_r(\text{MPa}) = 7.73 \times 10^4 [f(\psi)]^{-1.34} f_i(\sigma)^{0.35}$	262	0.78	0.17	15
<b>Taxiway B</b>						
Thawed base/subbase	FWD/RPB	$\dagger M_r(\text{MPa}) = 5.55 \times 10^{10} [f(\psi)]^{-4.72} f_i(\sigma)^{0.27}$	173	0.69	0.26	16
		$M_r(\text{MPa}) = 9.67 \times 10^9 [f(\psi)]^{-4.36} f_i(\sigma)^{0.36}$	173	0.73	0.24	17
		$M_r(\text{MPa}) = 4.28 \times 10^6 [f(\psi)]^{-3.99} f_i(\sigma)^{0.27} f(\gamma_d)^{8.35}$	173	0.71	0.25	18
		$M_r(\text{MPa}) = 1.56 \times 10^6 [f(\psi)]^{-3.69} f_i(\sigma)^{0.36} f(\gamma_d)^{7.72}$	173	0.74	0.23	19
Frozen base/subbase		$\dagger M_r(\text{MPa}) = 1.00 \times 10^3 (w_u/w_t)^{-2.63}, w_u = 3 \times 10^{-2}(-T)^{-0.22}, w_t = 0.05$	92	0.96	0.42	20
Thawed subgrade	FWD/RPB	$\dagger M_r(\text{MPa}) = 8.76 \times 10^4 [f(\psi)]^{-2.38} f_i(\sigma)^{0.30}$	293	0.72	0.20	21
		$M_r(\text{MPa}) = 3.36 \times 10^4 [f(\psi)]^{-2.15} f_i(\sigma)^{0.34}$	293	0.68	0.21	22
		$M_r(\text{MPa}) = 3.80 \times 10^6 [f(\psi)]^{-2.36} f_i(\sigma)^{-3.25} f(\gamma_d)^{-3.06}$	293	0.74	0.19	23
		$M_r(\text{MPa}) = 1.35 \times 10^6 [f(\psi)]^{-2.13} f_i(\sigma)^{0.34} f(\gamma_d)^{-3.06}$	293	0.70	0.20	24
Frozen subgrade		$M_r(\text{MPa}) = 2.66 (w_u/w_t)^{-1.02} f_i(\sigma)^{0.78}, w_u = 3.14 \times 10^{-2}(-T)^{-0.29}, w_t = 0.29$	152	0.82	0.92	25
		$M_r(\text{MPa}) = 2.59 (w_u/w_t)^{-0.83} f_i(\sigma)^{0.93}, w_u = 3.14 \times 10^{-2}(-T)^{-0.29}, w_t = 0.29$	152	0.84	0.85	26
Frozen subgrade		$M_r(\text{MPa}) = 3.31 \times 10^4 (w_u/w_t)^{-0.87} f_i(\sigma)^{0.68}, w_u = 3.14 \times 10^{-2}(-T)^{-0.29}, w_t = 0.29$	152	0.82	0.92	27
		$M_r(\text{MPa}) = 2.66 (w_u/w_t)^{-1.02} f_i(\sigma)^{0.78}, w_u = 3.14 \times 10^{-2}(-T)^{-0.29}, w_t = 0.29$	152	0.82	0.92	25
Frozen subgrade		$M_r(\text{MPa}) = 2.59 (w_u/w_t)^{-0.83} f_i(\sigma)^{0.93}, w_u = 3.14 \times 10^{-2}(-T)^{-0.29}, w_t = 0.29$	152	0.84	0.85	26
		$M_r(\text{MPa}) = 3.31 \times 10^4 (w_u/w_t)^{-0.87} f_i(\sigma)^{0.68}, w_u = 3.14 \times 10^{-2}(-T)^{-0.29}, w_t = 0.29$	152	0.82	0.92	27
Nonfrozen subgrade		$M_r(\text{MPa}) = 5.16 \times 10^6 [f(\psi)]^{-2.71} f_i(\sigma)^{0.26}$	278	0.81	0.15	28
		$M_r(\text{MPa}) = 5.48 \times 10^6 [f(\psi)]^{-2.71} f_i(\sigma)^{0.26}$	278	0.72	0.18	29
		$M_r(\text{MPa}) = 2.49 \times 10^6 [f(\psi)]^{-2.73} f_i(\sigma)^{0.26} f(\gamma_d)^{2.07}$	278	0.82	0.14	30

NOTES:

RPB = repeated-load plate-bearing apparatus waveform

FWD = falling-weight deflectometer waveform

† = equations used in analysis

n = number of points

R<sup>2</sup> = coefficient of determination

M<sub>r</sub> = resilient modulus

T = θ/θ<sub>0</sub>

θ = temperature (°C)

θ<sub>0</sub> = 1 °C

f<sub>Hz</sub> = load waveform frequency (Hz)

f(ψ) = (101.36-ψ)/ψ<sub>0</sub>

ψ = moisture tension (kPa)

ψ<sub>0</sub> = 1 kPa

f<sub>i</sub>(σ) = (J<sub>i</sub>/σ<sub>0</sub>)

f<sub>i</sub>(σ) = (J<sub>i</sub>/τ<sub>oct</sub>)/σ<sub>0</sub>

f<sub>i</sub>(σ) = τ<sub>oct</sub>/σ<sub>0</sub>

σ = stress (kPa)

σ<sub>0</sub> = 1 kPa

J<sub>1</sub> = first stress invariant (kPa)

J<sub>2</sub> = second stress invariant (kPa)

τ<sub>oct</sub> = octahedral shear stress (kPa)

f(γ<sub>d</sub>) = γ<sub>d</sub>/γ<sub>0</sub>

γ<sub>d</sub> = dry unit weight (Mg/m<sup>3</sup>)

γ<sub>0</sub> = 1 Mg/m<sup>3</sup>

w<sub>u</sub> = unfrozen water content (decimal)

w<sub>t</sub> = total water content (decimal)

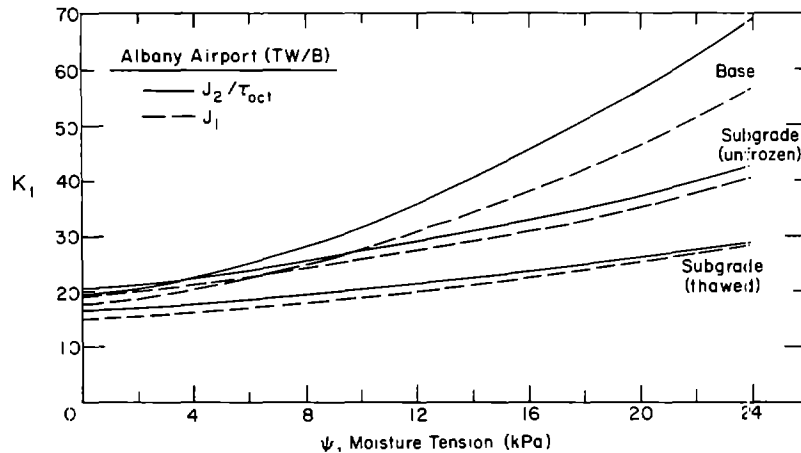


Figure 32. Coefficient  $K_1$  of the empirical models (eq 9 and 10) vs moisture tension for several soils from Taxiway B, Albany Airport.

### Field verification

Field in-situ data for the test sections from which the samples had been obtained were needed for two purposes. On the one hand it was desired to measure surface deflections under plate loads to compare with deflections calculated with the help of the laboratory-derived expressions for resilient modulus. This comparison could verify the validity of the laboratory testing methods. Field data were also needed to document the seasonal variation of temperature and moisture tension throughout a complete annual cycle. These variables significantly affect the resilient modulus, and their definition is essential for a time-dependent evaluation of the resilient modulus, which laboratory testing alone cannot provide.

### Deflection measurements

For measuring load-induced deflections, two types of in-situ tests were employed (Johnson et al. 1982). The first was a repeated-load plate-bearing (RPB) test. The equipment is mounted in the center of a large, enclosed semi-trailer. In our tests the load actuator applied pressures in the range from about 200 to 600 kPa through a 304-mm-diameter plate. The pulse duration was about 1 s and the cycle time was about 3 s. Pavement deflection was monitored at radial distances by means of LVDTs mounted on a reference beam.

The second type of in-situ test equipment was the falling-weight deflectometer (FWD). With this device a 28-ms pulsed load was applied to a 300-mm-diameter plate resting on the pavement surface. This load pulse simulated a truck wheel moving at moderate speed. The stress imposed ranged from 200 to 1700 kPa. The pavement deflection at ra-

dial distances from the load plate was monitored by means of velocity transducers.

The equipment described above was used at the Winchendon test sections on 22 occasions from October 1978 through April 1980. At Albany County Airport the same equipment was used on 12 occasions between November 1978 and June 1980. Between November 1982 and May 1983, FWD tests were performed 11 times at Albany County Airport.

The vertical resilient displacements obtained from the tests were plotted as deflection basins (Fig. 33). The displacements at the Winchendon test sections measured first in the autumn of 1978 (Fig. 5) decreased to small amounts in the second series of tests, made in February 1979 when the test soils were frozen. The plots show the sharp increase in displacement after thawing started. The increase in surface deflection upon thawing was particularly great for the four test soils at Winchendon containing the greatest fractions of fines (material passing the No. 200 sieve), the Ikalanian, Graves and Hyannis sands and the Sibley till. Even in these soils a substantial decrease in deflection (recovery) was observed within 10–20 days after thawing started. In the Hart Brothers sand and the dense-graded stone the increased deflection upon thawing did not differ greatly from the autumn (recovered) deflection. The comparative response of the six soils to thawing is illustrated in Figure 34.

Similar plots for the pavements at Albany County Airport also show the sharp increase in displacement after thawing starts (Fig. 12). At Taxiway A, however, the displacement during thawing was not much higher than that recorded

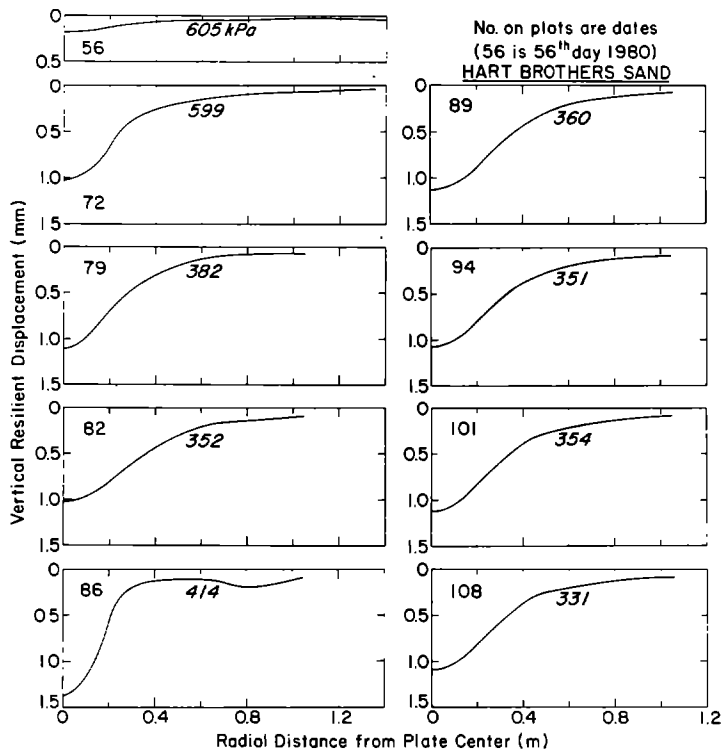


Figure 33. Deflection basins measured in 1980 FWD test, Hart Brothers sand test section.

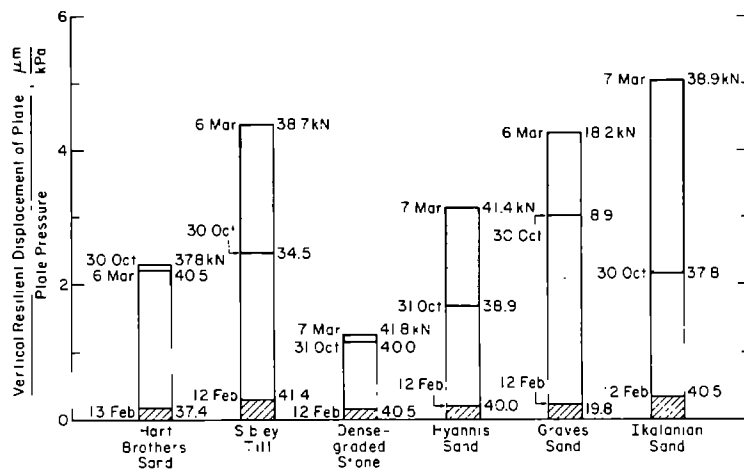


Figure 34. Vertical resilient displacement observed on six test sections prior to freezing (October 1978), while frozen (February 1979) and during thawing (March 1979). Plate loads are shown in kilonewtons.



the previous November, and it tended to increase on the dates succeeding the thaw, probably reflecting a stronger dependence on the temperature of the thick asphalt concrete pavement than on the condition of the base or subbase.

#### Analytical approach

The objective in analyzing the plate-bearing tests was to calculate the deflection basin resulting from the application of a known load, using for each layer the linear or nonlinear resilient modulus and Poisson's ratio determined in advance by laboratory tests. Comparison of the calculated deflection basins with the basins actually observed in field tests permitted laboratory test procedures to be validated. The computer program for analyzing nonlinear elastic layered systems (NELAPAV) chosen for the calculation of deflections was developed by Irwin (Irwin and Johnson 1981) as a modification of the CHEVRON code.

NELAPAV incorporates five basic models of resilient-modulus stress dependency. Any one of these models could be selected for any pavement layer. The models include

$$\text{Type 1: } M_r = \text{constant}$$

$$\text{Type 2: } M_r = K_1 J_1^{K_2}$$

$$\text{Type 3: } M_r = K_2 + (K_1 - \sigma_d) K_3, \sigma_d < K_1$$

$$M_r = K_2 + (\sigma_d - K_1) K_4, \sigma_d > K_1$$

$$\text{Type 4: } M_r = K_1 (J_2 / \tau_{\text{oct}})^{K_2}$$

$$\text{Type 5: } M_r = K_1 (\tau_{\text{oct}})^{K_2}$$

where  $K_1$ ,  $K_2$ ,  $K_3$  and  $K_4$  are regression constants. In analyzing the six Winchendon test sections, we used the type 1 model for the asphalt concrete, types 1, 4 and 5 for the frozen test soils, and types 2 and 4 for the thawed and recovered test soils and the natural subgrade test soil. As the analyses proceeded, the type 4 model became preferred over the type 2 model for thawed soils. In analyzing the deflection on Taxiways A and B, the type 1 model was used for asphalt concrete and for frozen base, while the type 4 model was used in all other cases.

In addition to selecting a model for the resilient modulus and inputting the applicable values for the regression constants, we selected appropriate values for the resilient Poisson's ratio from experience with other materials and from published test data (Table 6).

Another important parameter that the user must select for each layer is the coefficient of lateral earth pressure at rest  $K_0$ , which is used in calculating the stresses generated by the weights of the layers overlying the point for which the calculations are being made. Values chosen for  $K_0$  at the Winchendon test sections were 1.5 for the asphalt concrete and subgrade and 1.0 for the test soils. For the analysis of deflections at Taxiways A and B, to preclude instability of the stress function, we chose  $K_0$  values of 1.0 for the asphalt concrete and subgrade and 0.7 for the base and subbase.

#### Calculated deflections compared with measurements

For the deflection calculations the temperatures and moisture tensions prevailing in the pavements at the time of each test, together with the plate pressures measured for each test, were taken as given values, and the stress-dependency model appropriate to each layer was selected. NELAPAV calculated stresses, strains, displacements and stress-compatible moduli throughout the system.

The comparisons between the calculated and measured deflections at Winchendon for the highest plate loading are summarized in Figure 35 for three of the test sections; the comparison is similar for the other test sections and for the lower loads (Johnson et al. 1986a). Several general trends are apparent in these plots. The maximum deflections at the basin's center, calculated by NELAPAV, tend to agree well with the maximum surface deflections measured in both the RPB and FWD tests, but they did not agree as well at the outer radii. The agreement is somewhat better for FWD tests (1980 data) than for RPB tests (1978-1979 data). Perhaps the most significant observation is

**Table 6. Values of Poisson's ratio used in analysis.**

Asphalt concrete	$T < -2^\circ\text{C}$	0.30	
	$-2 < T < +1$	0.35	
	$+1 < T < +8$	0.40	
	$+8 < T < +16$	0.45	
	$T > +16$		
Test soils			
	Frozen	0.30-0.35	
	Thawed	$\psi < 2$ (to 4) kPa	0.45
		$2$ (to 4) $< \psi < 8$ (to 10)	0.40
$\psi > 8$ (to 10)		0.35	
Subgrade		0.35	

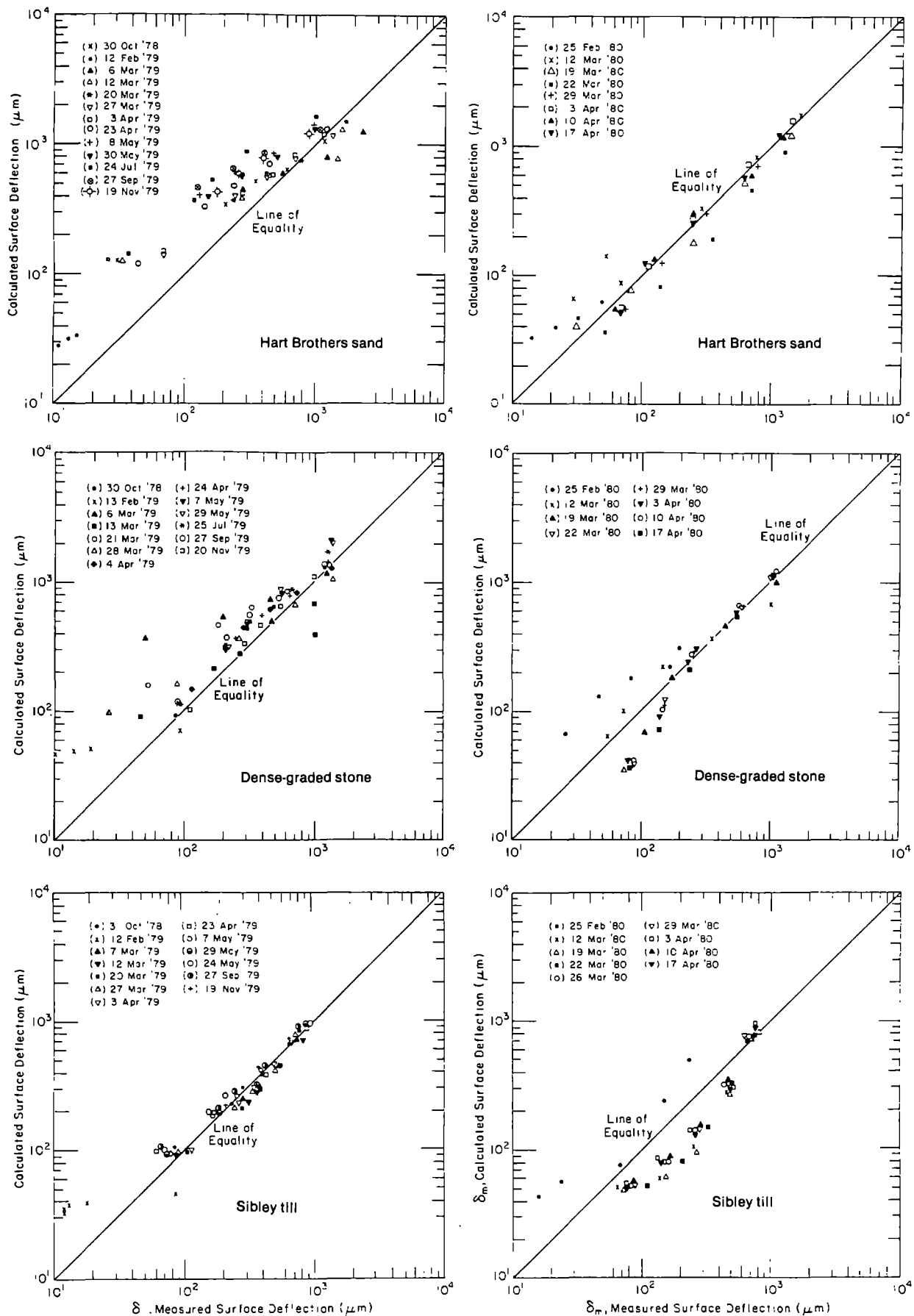


Figure 35. Measured surface deflections compared with deflections calculated by NELPAV for three test sections.



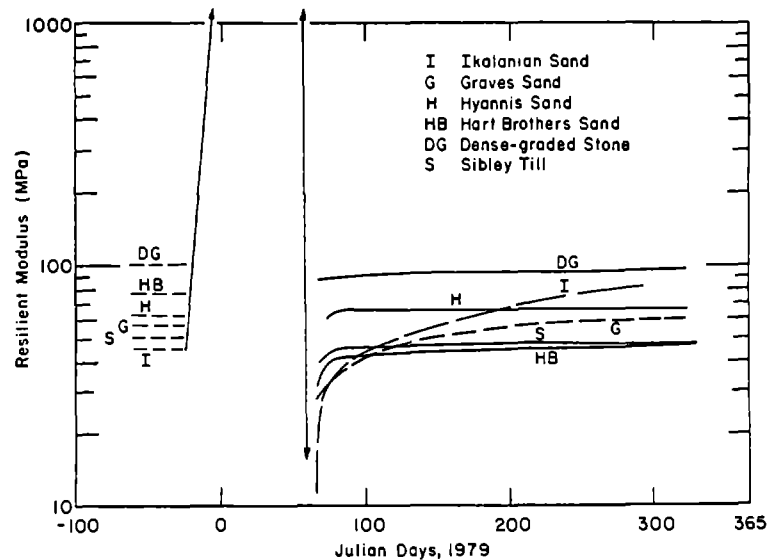


Figure 37. Interpretation of seasonal variation in the resilient modulus of six test soils directly beneath asphalt pavement.

the reasonably good agreement of the post-thaw basins in general. The calculated and measured deflections differ more when the cross section included layers of frozen soil. This problem can be attributed in part to uncertainties in defining the exact thickness of the frozen layers.

The comparisons between the calculated and measured deflections (FWD tests) for Taxiway A test point N2 and Taxiway B test point T5 are shown in Figure 36. Corresponding plots for the other test points of Taxiway A are given by Johnson et al. (1986b). Agreement is excellent.

The calculated resilient moduli and other results from the analysis of the test sections are summarized by Johnson et al. (1986a, b). The resilient moduli of the test soils calculated by NELAPAV show the expected seasonal variation: extremely high values in the frozen condition, decreasing dramatically upon thawing and increasing somewhat during the late spring, summer and fall. An interpretation of the variation in modulus of the upper layer of each test soil under the lower of the test loads is given in Figure 37 for the Winchendon test sections. Figures 38 and 39 show similar interpretations for the various layers in Taxiways A and B at Albany County Airport.

The agreement of the calculated deflections with the deflections measured under FWD loading is strong evidence that the equations for nonlinear resilient modulus developed from laboratory triaxial tests represent valid characterizations of the materials in the layered pavement system. Accord-

ingly the procedures for the laboratory repeated-load triaxial tests, including testing at successive levels of moisture tension to track the recovery process in thaw-weakened soils, are considered to be valid. Those procedures should be useful for structural evaluation and design of pavements affected by freezing and thawing.

This investigation has demonstrated that the resilient modulus depends strongly on the temperature and moisture tension. These seasonally varying parameters can be evaluated by installing sensors at various depths below a paved surface and collecting data over a complete annual cycle. Alternatively the frost-heave model of Guymon et al. (in prep.) can be used to predict both temperatures and moisture tension as variables in time and space.

#### Summary of predictive approach

This research has defined and verified an approach for evaluating the resilient modulus of granular subgrade and base course materials as a variable in time and space. While the principal focus of the work was seasonal variation, the space variable, represented by the position of a material in the pavement profile, also proved to be significant, not only because seasonal variation in temperature and moisture tension itself depends on depth, but because depth below the pavement surface also is a determinant of stress, which in a granular material strongly governs its resilient modulus. Pavement design and evaluation are af-

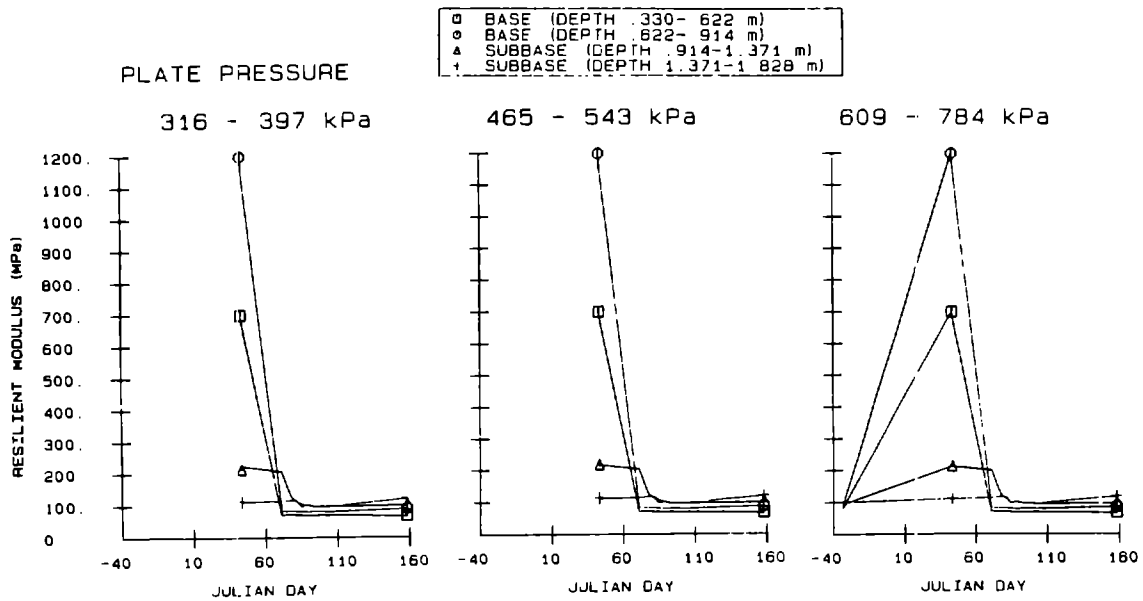


Figure 38. Seasonal variation in the resilient modulus of the base and subbase at radius 0.0, Taxiway A, test point C4, 1979-80.

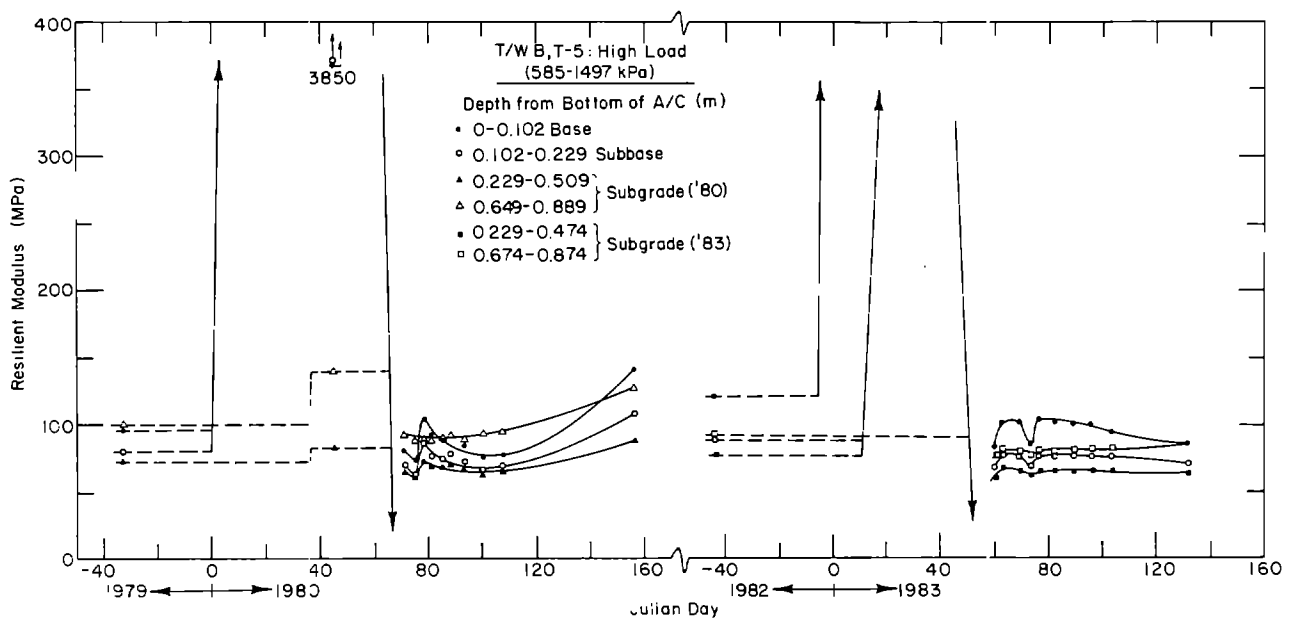


Figure 39. Seasonal variation in the resilient modulus of the base, subbase and subgrade at radius 0.0, Taxiway B, test point T5, high load, 1979-80 and 1980-83.

affected principally by the variation in resilient modulus between early spring, when thawing first begins, and late fall, when the materials freeze. Laboratory testing, essential for predicting the resilient modulus throughout this period, should start with frozen samples. The following is a summary of the approach:

- Obtain undisturbed frozen samples from the site in late winter, or prepare compacted specimens in the laboratory and freeze them under controlled conditions similar to the natural environment.
- Allow specimens to thaw within a triaxial test chamber, and perform repeated-load

triaxial tests at various levels of confining pressure and deviator stress equivalent to the range of stresses expected within the pavement. Monitor axial and radial recoverable and permanent strain, as well as stress levels.

- Successively desaturate the specimens through a range of levels of moisture tension, conducting repeated-load tests at each level. Measure the moisture tension before each test.
- Through multiple linear regression techniques, develop equations for characterizing the resilient modulus in terms of an appropriate stress function; moisture tension, and possible dry density, should be included as independent variables.
- Evaluate the seasonal variation of moisture tension in the existing or planned pavement substructure. The evaluation can be made by implanting tensiometers beneath the existing pavement, or a similar pavement nearby, and monitoring them throughout one full year. Alternatively the frost heave model can be used to predict the variation in moisture tension throughout the thawing and recovery period.
- The characterization of the seasonal variation in the modulus is essentially complete with the development of the regression equations outlined above and the evaluation of the moisture tension as a time-dependent variable. The resilient modulus at a particular time and under particular traffic loading conditions can be evaluated numerically as part of the analysis of the pavement cross section. A suitable pavement response model would be used to calculate the stresses and the stress-compatible moduli, as well as other outputs such as strain and displacement.

#### **SIMULATING FROST HEAVE AND PAVEMENT DEFLECTION**

The mathematical model for frost heave and thaw consolidation and the nonlinear layered elastic pavement response model NELAPAV, in concert with the results of laboratory resilient-modulus tests, were used to simulate frost heave and pavement deflection in the field. Comparison with field observations provided the ultimate test of the modeling and laboratory testing procedures.

Calculations were made with the one-dimensional mathematical model to simulate the frost heave and thaw consolidation at the field test sites. The time-dependent temperatures and pore pressures calculated for nodal points within the pavement substructure were used to determine unique layers within the freezing or thawing system and to select equations characterizing the resilient modulus of each layer. The appropriate equations for resilient modulus were then input into the NELAPAV program along with temperatures and pore pressures (moisture tension), and the deformations and stresses at each point of interest were calculated. The test of the efficacy of the procedure required a comparison of the observed and calculated frost heave, and the seasonal variation of pavement deflection under repeated loading.

#### **Method of evaluation**

The procedure for calculating the frost heave and pavement deflection was as follows. For a particular test section, the appropriate boundary conditions and material properties were input into the frost-heave model. Repeated simulations with varying values of the correction factor  $E$  were conducted with the mathematical model until the calculated frost-heave values agreed with the field values. The frost depth and frost heave (or thaw depth and thaw settlement) and the temperature and pore-water pressure (or tension) were then printed out on a daily basis. The soil profile for each day was divided into frozen and thawed zones. The thawed zone was further divided into layers according to moisture tension, and the frozen zone was divided into layers according to temperature. Because the moisture tension or temperature varied within each layer, average values were calculated. Next, the appropriate expressions for the temperature-dependent or moisture-stress-dependent resilient modulus  $M_r$  were selected for the frozen and thawed soil and the asphalt concrete from the array of equations given in Tables 4 and 5.

The appropriate models of stress dependency contained within NELAPAV were selected, the regression coefficients and other layer data were input into the NELAPAV program for each layer, and the pavement deflection under a 260-kPa applied stress was calculated for each day or time interval during which significant changes occurred within the pavement test section.

#### **Results and discussion**

Figure 40 shows the results for the Graves sand

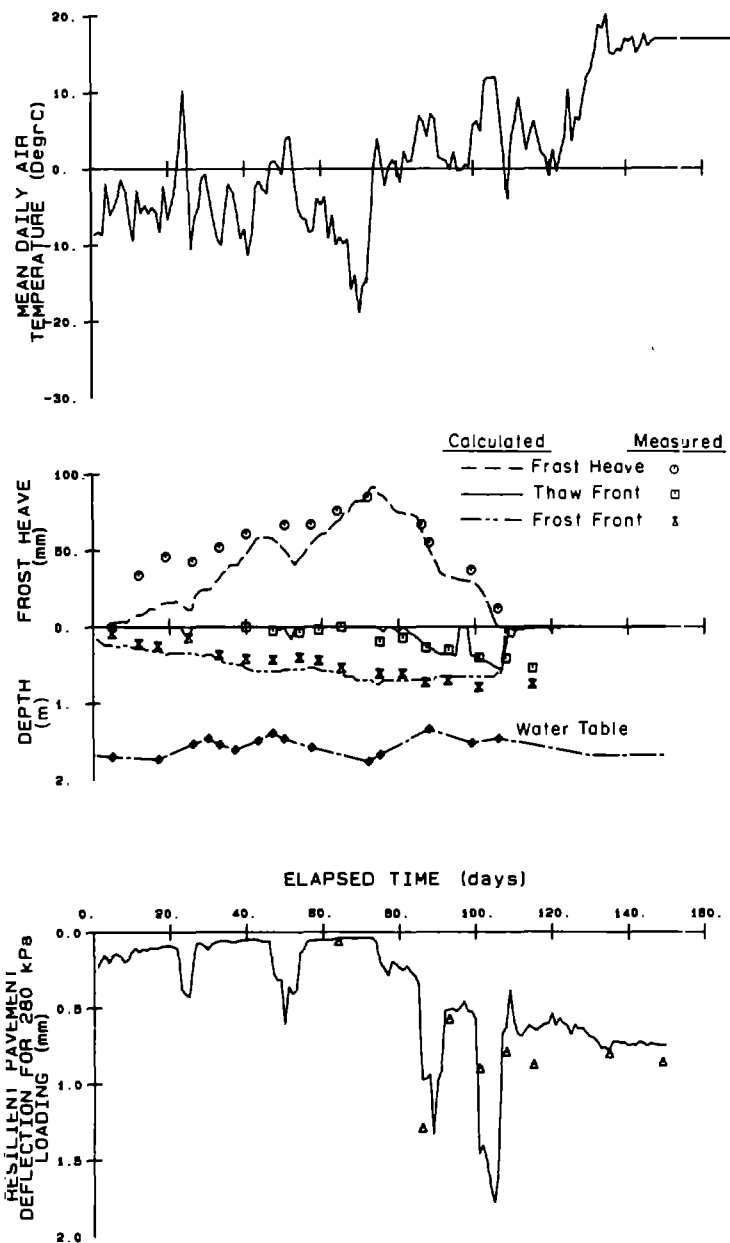


Figure 40. Comparison of simulated frost heave, frost and thaw depths, and pavement deflection with field observations, Graves sand test section, 1978-79.

test section at the Wirchendon site. The calculated pavement deflections agree well with the measured values. The predictions made to date with this procedure demonstrate the efficacy of the frost-heave and thaw-consolidation model and the nonlinear layered elastic pavement response model for calculations of seasonal frost heave and pavement deflection under load. The models thus provide an instrument for implementing much of the work performed under this multi-phase research project.

It is still necessary, however, to adjust the  $E$  factor in the mathematical model of frost heave to make the calculated and observed values of frost heave agree. We expect that after more experience is gained with the frost-heave model a correlation between  $E$  and a soil factor such as particle size will be found and that eventually  $E$  values will be available as a chart or nomograph.

Once the appropriate  $E$  factor is selected, there appear to be no more significant limitations on the use of this method to predict frost heave, thaw set-

tlement and pavement deflection under wheel loading. A distinct advantage of this approach is that the final results make it possible to apply modern pavement-design systems including mechanistic analysis and a cumulative-damage approach.

## **SUMMARY OF FINDINGS**

### **Frost-susceptibility index tests**

A comprehensive review of the existing frost-susceptibility index tests led to the selection of the three most promising methods. After further evaluation, development of new methods, testing and comparison with field observations, two methods of differing levels of complexity were found to be useful as indicators of field performance. The Corps of Engineers frost design soil classification method, comprising very simple test procedures, is useful for separating non-frost-susceptible from frost-susceptible soils, but it does not reliably identify their degrees of susceptibility to frost heave nor is it effective for predicting the degree of thaw-weakening susceptibility. At a much higher level of complexity, a newly developed freezing test can be used to determine the frost-heave susceptibility in the field, and the CBR value after thawing is a strong indicator of field thaw weakening leading to increased resilient deflection under applied loads.

### **Soil column and dual gamma system**

A soil column and dual gamma system were developed for use as research instruments for obtaining data on the changes in soil moisture content and density that occur during freezing and thawing. The results from tests on soils from Winchendon and other sites were used for improving and validating the frost-heave model. The devices also made it possible to conduct two special tests used to validate the thaw-settlement algorithm of the frost-heave model.

### **Mathematical model of frost heave and thaw settlement**

A model developed under an earlier cooperative research project was improved, refined and extended. The refinements were introduced as verification work progressed; they included accurate simulations of pore pressures, temperatures and frost heave. Major extensions to the model included the addition of a thaw-settlement algorithm and a probabilistic component that accounted for

variations in the hydraulic conductivity caused by spatial and temporal variations in soil properties.

The model was tested by running computer simulations of the test sections at Winchendon, Massachusetts, and at Albany County Airport, New York. The calculated frost depths, frost heaves and thaw settlements were compared with field observations at the test sections.

In general the results show that good results can be obtained from the model for soils ranging from silts to relatively coarse-grained and only marginally frost-susceptible soils. The model must be calibrated, however, to achieve such results. This is done by adjusting the value for hydraulic conductivity in the freezing zone. We believe that the model simulates freezing processes adequately for engineering purposes. Model outputs include frost heave at the pavement surface and subsurface temperature and pore-water-pressure distributions with depth, all of which are directly useful in the pavement design process.

### **Seasonal variation in resilient modulus of granular soils**

The objective of this phase of the work was to develop laboratory methods for characterizing the seasonal changes in the resilient modulus of granular soils throughout a complete annual cycle of freezing, thawing (and accompanying loss of supporting capacity) and recovery from the weakened condition. A laboratory testing method was developed for conducting repeated-load triaxial tests on a sample initially in the frozen state, continuing the load repetitions after the sample thawed, and resuming load repetitions again at successively increased levels of moisture tension obtained by progressive desaturation of the sample.

Tests using this method were completed on 11 soils from paved areas at test sites at Winchendon, Massachusetts, and Albany County Airport, New York. By means of multiple regression analysis of the test results, the resilient modulus of each soil was expressed in terms of the governing parameters. The main parameter for soils in the frozen state is temperature, while the resilient modulus of soils in the thawed and recovering states depends mainly on the applied stress and the moisture tension.

The validity of the method was tested by using the expressions for resilient modulus to calculate resilient deflections under plate loads at the two test sites and then measuring the actual deflections produced by a falling-weight deflectometer or in some cases by a repeated-load plate-bearing de-



vice. Agreement was good between the calculated and measured deflections. Accordingly, it is concluded that the laboratory test method, supplemented by soil-moisture-tension and temperature data obtained from field measurements or predicted by the frost-heave model, can provide evaluations of seasonal variations of the resilient modulus of granular soils and base courses.

## IMPLEMENTATION OF RESEARCH FINDINGS

Investigations in the principal study areas have produced results that can be advantageously used in designing and evaluating pavements in frost areas. The examination of frost-susceptibility index tests (Chamberlain, in prep. a) identified the Corps of Engineers frost design soil classification system and a new laboratory freeze-thaw test as two levels of testing that should be put in practice. The frost-heave model can be implemented beneficially in any system for pavement design or evaluation. And finally, the laboratory repeated-load triaxial test on thawed and recovering soil can not only be implemented in mechanistic design or evaluation systems, but when used with either the frost-heave model or with in-situ measurements of values of moisture tension, it can be implemented in systems employing a cumulative damage approach. The scope and extent of the implementation of each of the research findings, and its potential impact on pavement design and evaluation, depend on the type of system that is in use for pavement analysis.

### Corps of Engineers frost design soil classification system

This frost-susceptibility classification system (Table 1), based on simple classification tests, leads to the assignment of a frost group number to each soil. Its implementation (Fig. 41) is limited to those pavement design or evaluation systems that are based on the frost group number.

### New laboratory freeze-thaw test

This improved freezing test incorporates a CBR test on the thawed specimen. Outputs (Fig. 42) are heave rate from the freezing phase, and CBR in the thawed state; scales of susceptibility to frost heave and to thaw weakening may be derived from these outputs (Table 3). Frost-heave susceptibility can be applied effectively, as an indication of potential roughness, to any mechanistic or empirical

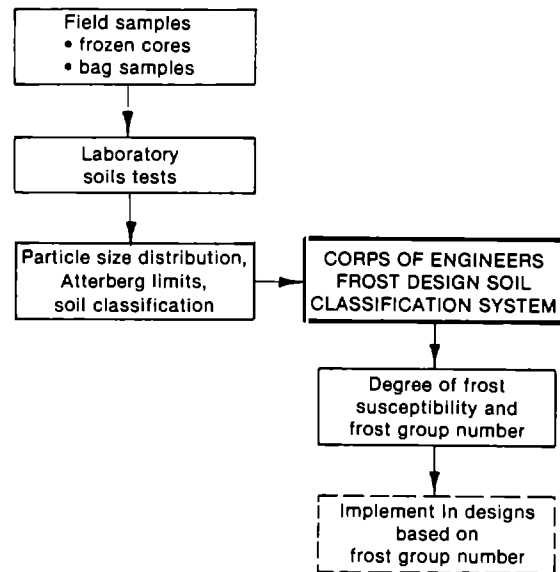


Figure 41. Implementation of the Corps of Engineers frost design soil classification system.

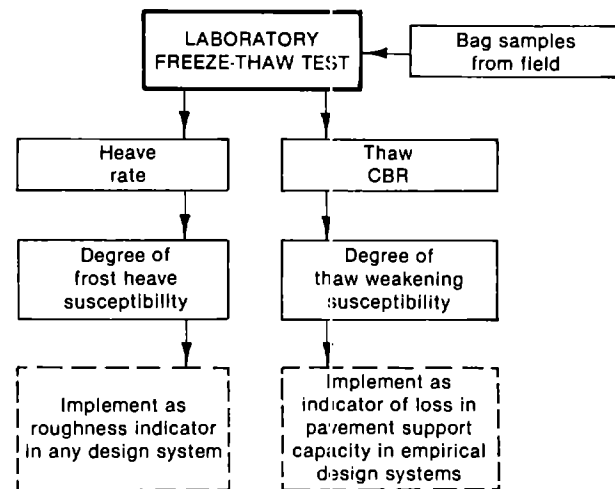


Figure 42. Implementation of the new freeze test.

design or evaluation system. The classification of susceptibility to thaw weakening can be used as an indicator of seasonal (spring) loss of support as part of any empirical design or evaluation system. In developing a pavement design these indicators would be used as adjustments to design thicknesses determined by other types of analyses.

### Frost-heave model

The frost-heave model provides for the first time an ability to calculate with reasonable confidence the magnitude of the heave that can be expected in a given pavement cross section under

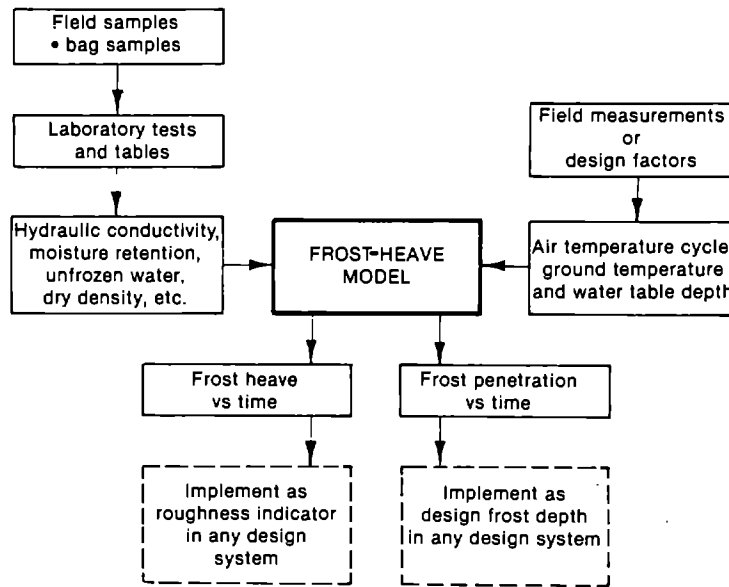


Figure 43. Implementation of the frost-heave model.

prescribed climatic, geotechnical and hydraulic conditions. Since the outputs of depth of frost and magnitude of heave (Fig. 43) are referenced to a particular point on the pavement where conditions are known, the model does not predict pavement roughness. Heave at a point can be used as an indicator of potential roughness, however, and can be implemented as an adjunct to any pavement design or evaluation system. For example, the calculated frost heave might serve as a basis for adjusting a trial design thickness if necessary to reduce the expected winter pavement roughness. The second principal output from the model, the predicted depth of frost beneath a pavement having a certain trial cross section, can be used as direct input for those design systems in which the total thickness of the pavement section depends on the depth of frost. It can also be used as an adjunct to any design system.

**Repeated-load triaxial test on frozen and thawed soil**

The repeated-load triaxial test on frozen and thawed specimens provides a means of evaluating the resilient modulus of subgrade and base soils at various stages during the freeze-thaw-recovery cycle. The regression equations for soil in the thawed state (Fig. 44) are of the greatest interest, as in many cases they represent the condition having the lowest resilient modulus and consequently the greatest potential for pavement distress. The expressions for resilient modulus can be imple-

mented directly in any mechanistic design or evaluation system that employs a multilayered or finite-element simulation model formulated to analyze nonlinear materials.

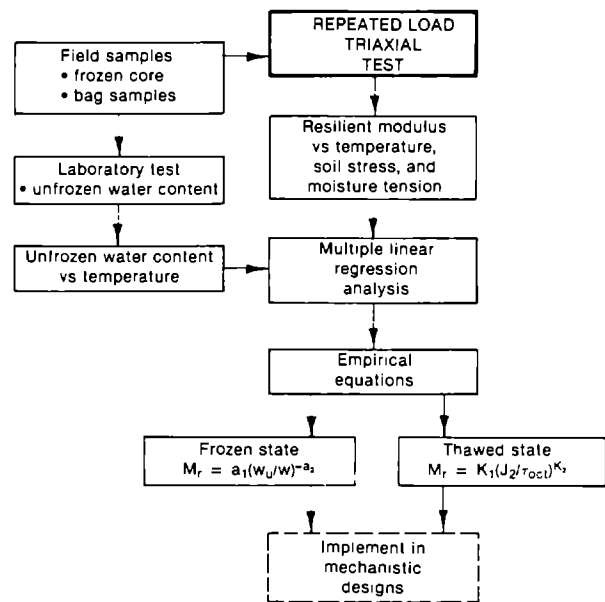


Figure 44. Implementation of the repeated-load triaxial test for stress-strain-deflection analysis.

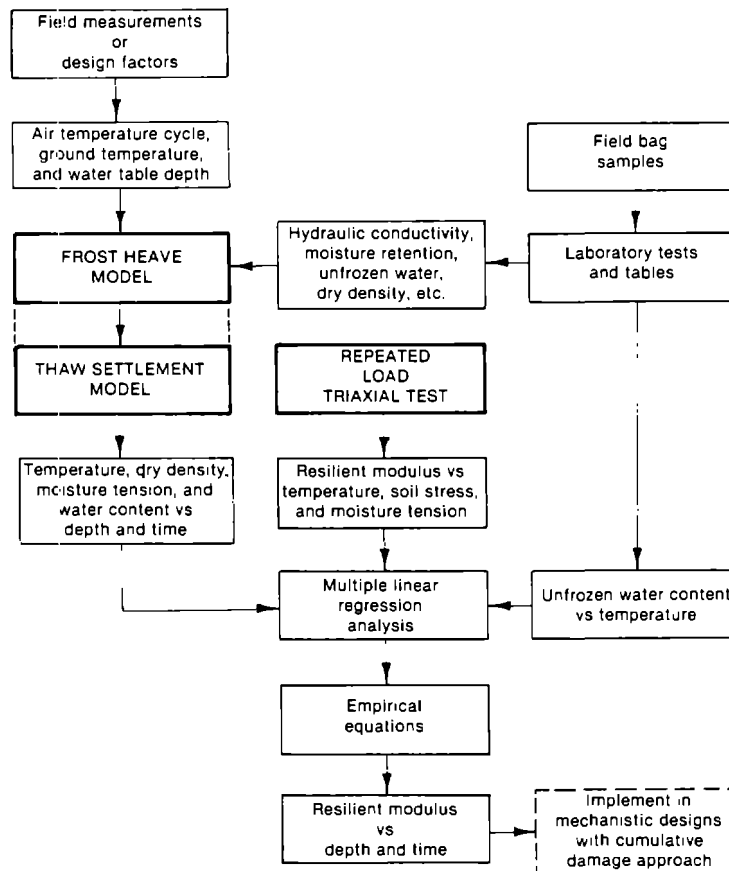


Figure 45. Implementation of the seasonally varying resilient modulus for stress-strain-deflection analysis with a cumulative damage approach.

### Evaluation of seasonal variation of resilient modulus

It is unrealistic to base the design or evaluation of a pavement on only the lowest resilient modulus value reached during the year (usually during thawing), and there is no reasonable basis for selecting any other single value to serve as an annual average representative of all the seasons. Rather, methods that include a cumulative damage approach, currently coming into greater use, offer the advantage of more rigorously assessing the effect of the complete annual cycle of freezing, thawing and recovery. Application of these methods requires that the resilient modulus be expressed as a function of time, so that the pavement performance can be analyzed by dividing the year into discrete intervals during which the modulus may be assumed to be constant. The evaluation of seasonal variations of the resilient modulus requires that the modulus be characterized in terms of the moisture tension and that the seasonal vari-

ation of the moisture tension be monitored or predicted. Figure 45 shows that repeated-load triaxial tests can be used to measure the resilient modulus as a function of temperature, soil stress and moisture tension. The frost-heave model and its associated thaw-settlement model are used to predict the key parameters of temperature and moisture tension as variables in time and space. With this linkage the resilient modulus at various depths is defined as a continuous function of time, facilitating the application of mechanistic analyses for pavement design and evaluation using a cumulative damage approach.

### LITERATURE CITED

Berg, R.L., G.L. Guymon and T.C. Johnson (1980a) Mathematical model to correlate frost heave of pavements with laboratory predictions. USA Cold Regions Research and Engineering

- Laboratory, CRREL Report 80-10, 49 pp.
- Berg, R.L., J. Ingersoll and G.L. Guymon** (1980b) Frost heave in an instrumented soil column. *Cold Regions Science and Technology*, 3(2 and 3): 211-221.
- Berg, R.L. and T.C. Johnson** (1983) Revised procedure for pavement design under seasonal frost conditions. USA Cold Regions Research and Engineering Laboratory, Special Report 83-27, 129 pp.
- Chamberlain, E.J.** (1981a) Frost susceptibility of soil: Review of index tests. USA Cold Regions Research and Engineering Laboratory, CRREL Monograph 81-2, 121 pp.
- Chamberlain, E.J.** (1981b) Comparative evaluation of frost susceptibility tests. Transportation Research Board, Transportation Research Record 809, pp. 42-52.
- Chamberlain, E.J.** (In Prep. a) Evaluation of selected frost susceptibility test methods. USA Cold Regions Research and Engineering Laboratory, CRREL Report.
- Chamberlain, E.J.** (In Prep. b) A freeze-thaw test to determine the frost susceptibility of soils. USA Cold Regions Research and Engineering Laboratory, Special Report. Also U.S. Department of Transportation, Federal Aviation Administration Report DOT/FAA/PM-85/20.
- Chamberlain, E.J. and D.M. Carbee** (1981) The CRREL frost heave test. *Frost i Jord*, (22): 55-62.
- Chamberlain, E.J., P.N. Gaskin, D. Esch and R.L. Berg** (1984) Survey of methods for classifying frost susceptibility. In *Frost Action and Its Control*. American Society of Civil Engineers, Technical Council on Cold Regions Engineering Monograph, pp. 105-142.
- Cole, D.M.** (1984) Modeling the resilient behavior of frozen soil using unfrozen water content. In *Proceedings of the Third International Specialty Conference on Cold Regions Engineering, April 4-6, Edmonton, Alberta*, pp. 823-834..
- Cole, D.M., D. Bentley, G. Durell and T.C. Johnson** (1986) Resilient modulus of freeze-thaw affected granular soils for pavement design and evaluation. Part 1: Laboratory tests on soils from Winchendon, Massachusetts, test sections. USA Cold Regions Research and Engineering Laboratory, Hanover, N.H., CRREL Report 86-4. Also U.S. Department of Transportation, Federal Aviation Administration Report DOT/FAA/PM-84/16,1.
- Cole, D.M., D. Bentley, G. Durell and T.C. Johnson** (In Prep.) Resilient modulus of freeze-thaw affected granular soils for pavement design and evaluation. Part 3: Laboratory tests on soils from Albany County Airport. USA Cold Regions Research and Engineering Laboratory, Hanover, N.H., CRREL Report. Also U.S. Department of Transportation, Federal Aviation Administration Report DOT/FAA/PM-84/16,3.
- Cole, D.M., L.H. Irwin and T.C. Johnson** (1981) Effect of freezing and thawing on resilient modulus of a granular soil exhibiting non-linear behavior. Transportation Research Board, Transportation Research Record No. 809, pp. 19-26.
- DiMillio, A.F. and D.G. Fohs** (1980) The frost action problem—An overview of research to provide solutions. *Public Roads*, 43(4): March.
- Gardner, W.R.** (1958) Some steady-state solutions of the unsaturated moisture flow equation with application to evaporation from a water table. *Soil Science*, 85: 223-232.
- Greatorox, A.R., W.N. Tobiasson and R.L. Berg** (In Prep.) Design, fabrication and operation of a dual gamma system. USA Cold Regions Research and Engineering Laboratory, Hanover, N.H., CRREL Report.
- Guymon, G.L., T.V. Hromadka II and R.L. Berg** (1980) A one-dimensional frost heave model based upon simulation of simultaneous heat and water flux. *Cold Regions Science and Technology*, 3(2 and 3): 253-263.
- Guymon, G.L., R.L. Berg, T.C. Johnson and T.V. Hromadka II** (1981a) Results from a mathematical model of frost heave. Transportation Research Board, Transportation Research Record 809, pp. 2-6.
- Guymon, G.L., M.E. Harr, R.L. Berg, and T.V. Hromadka II** (1981b) Probabilistic-deterministic analysis of one-dimensional ice segregation in a freezing soil column. *Cold Regions Science and Technology*, 5: 127-140.
- Guymon, G.L., R.L. Berg, T.C. Johnson and T.V. Hromadka II** (In Prep.) Mathematical model of frost heave and thaw settlement in pavements. USA Cold Regions Research and Engineering Laboratory, Hanover, N.H., CRREL Report. Also U.S. Department of Transportation, Federal Aviation Administration Report DOT/FAA/PM-86/27.
- Hromadka, T.V. II, G.L. Guymon and R.L. Berg** (1981) Some approaches to modeling phase change in freezing soils. *Cold Regions Science and Technology*, 4: 137-145.
- Hromadka, T.V. II, G.L. Guymon and R.L. Berg** (1982) Sensitivity of a frost heave model to numerical method. *Cold Regions Science and Technology*, 6:1-10.

**Irwin, L.H. and T.C. Johnson** (1981) Frost-affected resilient moduli evaluated with the aid of nondestructively measured pavement surface deflections. Paper presented to Transportation Research Board Task Force on "Nondestructive Evaluation of Airfield Pavements."

**Jame, Y.-W.** (1978) Heat and mass transfer in freezing unsaturated soil. Ph.D. Dissertation, University of Saskatchewan, Saskatoon, Canada.

**Johnson, T.C., R.L. Berg, K.L. Carey and C.W. Kaplar** (1975) Roadway design in seasonal frost areas. USA Cold Regions Research and Engineering Laboratory, Hanover, N.H., Technical Report 259. Also Transportation Research Board Synthesis of Highway Practice No. 26.

**Johnson, T.C., D.M. Cole and L.H. Irwin** (1982) Characterization of freeze-thaw affected granular soils for pavement evaluation. In *Proceedings, 5th International Conference on Structural Design of Asphalt Pavements, Amsterdam*. Vol. 1, pp. 805-817.

**Johnson, T.C., D. Bentley and D.M. Cole** (1986a) Resilient modulus of freeze-thaw affected granular soils for pavement design and evaluation. Part 2: Field validation tests at Winchendon, Massachusetts, test sections. USA Cold Regions Research and Engineering Laboratory, CRREL Re-

port 86-12. Also U.S. Department of Transportation, Federal Aviation Administration Report DOT/FAA/PM-84/16,2.

**Johnson, T.C., A. Crowe, M. Erickson and D.M. Cole** (1986b) Resilient modulus of freeze-thaw affected granular soils for pavement design and evaluation. Part 4: Field validation tests at Albany County Airport. USA Cold Regions Research and Engineering Laboratory, CRREL Report 86-13. Also U.S. Department of Transportation, Federal Aviation Administration Report DOT/FAA/PM-84/16,4.

**Kaplar, C.W.** (1974) Freezing test for evaluating relative frost susceptibility of various soils. USA Cold Regions Research and Engineering Laboratory, Hanover, N.H., Technical Report 250, 40 pp.

**Lambe, T.W. and R.V. Whitman** (1979) *Soil Mechanics, SI Version*. New York: John Wiley & Sons.

**Morgenstern, N.R. and J.F. Nixon** (1971) One-dimensional consolidation of thawing soils. *Canadian Geotechnical Journal*, **8**: 558-565.

**Taylor, G.S. and J.N. Luthin** (1978) A model for coupled heat and moisture transfer during soil freezing. *Canadian Geotechnical Journal*, **15**: 548-555.

